AEROSPACE REPORT NO.
ATR-2001(7595)-1

In-Field Monitoring of the Durability of Composite Materials

20 August 2001

Prepared by

G. F. HAWKINS, G. L. STECKEL, J. P. NOKES,
and J. L. BAUER
Space Materials Laboratory
Laboratory Operations

Prepared for

CALIFORNIA DEPARTMENT OF TRANSPORTATION
Sacramento, CA 94273-0001

Contract No. SA0A0111

Engineering and Technology Group

THE AEROSPACE CORPORATION
EL SEGUNDO, CALIFORNIA

LABORATORY OPERATIONS

The Aerospace Corporation functions as an "architect-engineer" for national security programs, specializing in advanced military space systems. The Corporation's Laboratory Operations supports the effective and timely development and operation of national security systems through scientific research and the application of advanced technology. Vital to the success of the Corporation is the technical staff's wide-ranging expertise and its ability to stay abreast of new technological developments and program support issues associated with rapidly evolving space systems. Contributing capabilities are provided by these individual organizations:

Electronics and Photonics Laboratory: Microelectronics, VLSI reliability, failure analysis, solid-state device physics, compound semiconductors, radiation effects, infrared and CCD detector devices, data storage and display technologies; lasers and electro-optics, solid state laser design, micro-optics, optical communications, and fiber optic sensors; atomic frequency standards, applied laser spectroscopy, laser chemistry, atmospheric propagation and beam control, LIDAR/LADAR remote sensing; solar cell and array testing and evaluation, battery electrochemistry, battery testing and evaluation.

Space Materials Laboratory: Evaluation and characterizations of new materials and processing techniques: metals, alloys, ceramics, polymers, thin films, and composites; development of advanced deposition processes; nondestructive evaluation, component failure analysis and reliability; structural mechanics, fracture mechanics, and stress corrosion; analysis and evaluation of materials at cryogenic and elevated temperatures; launch vehicle fluid mechanics, heat transfer and flight dynamics; aerothermodynamics; chemical and electric propulsion; environmental chemistry; combustion processes; space environment effects on materials, hardening and vulnerability assessment; contamination, thermal and structural control; lubrication and surface phenomena.

Space Science Applications Laboratory: Magnetospheric, auroral and cosmic ray physics, wave-particle interactions, magnetospheric plasma waves; atmospheric and ionospheric physics, density and composition of the upper atmosphere, remote sensing using atmospheric radiation; solar physics, infrared astronomy, infrared signature analysis; infrared surveillance, imaging, remote sensing, and hyperspectral imaging; effects of solar activity, magnetic storms and nuclear explosions on the Earth's atmosphere, ionosphere and magnetosphere; effects of electromagnetic and particulate radiations on space systems; space instrumentation, design fabrication and test; environmental chemistry, trace detection; atmospheric chemical reactions, atmospheric optics, light scattering, state-specific chemical reactions and radiative signatures of missile plumes.

Center for Microtechnology: Microelectromechanical systems (MEMS) for space applications; assessment of microtechnology space applications; laser micromachining; laser-surface physical and chemical interactions; micropropulsion; micro- and nanosatellite mission analysis; intelligent microinstruments for monitoring space and launch system environments.

Office of Spectral Applications: Multispectral and hyperspectral sensor development; data analysis and algorithm development; applications of multispectral and hyperspectral imagery to defense, civil space, commercial, and environmental missions.

1. REPORT NO.	2. GOVERNMENT ACCESSION NO.	3. RECIPIENT'S CATALOG NO.
ATR-2001(7595)-1		

4. TITLE AND SUBTITLE	5. REPORT DATE
In-Field Monitoring of the Durability of Composite Materials	Oct. 1, 2001
	6. PERFORMING ORGANIZATION CODE

7. AUTHOR(S)	8. PERFORMING ORGANIZATION REPORT NO.
G. F. Hawkins, G. S. Steckel, J. Nokes and J. Bauer	ATR-2001(7595)-1.

9. PERFORMING ORGANIZATION NAME AND ADDRESS	10. WORK UNIT NO.
The Aerospace Corporation Space Materials Laboratory P.O. Box 92957 Los Angeles CA 90009	11. CONTRACT OR GRANT NO. DTFH 71-98-PTP-CA-35

12. SPONSORING AGENCY NAME AND ADDRESS	13. TYPE OF REPORT & PERIOD COVERED
California Department of Transportation New Technology & Research, MS#83 P.O. Box 942873 Sacramento, CA. 94273-0001	Final Report
	14. SPONSORING AGENCY CODE

15. SUPPLEMENTARY NOTES

This project was performed in cooperation with the US Department of Transportation, Federal Highway Administration.

16. ABSTRACT

It has been demonstrated that composite column jackets can provide confinement, increase ductility and increase shear capacity in deficient bridge columns. Previous studies have produced durability data on the sensitivities of the various types of composites to environmental attack by addressing the material degradation issues related to environmental, physical and chemical concerns using accelerated testing techniques in laboratories. However, the performance of composites in actual bridge environments was still largely unknown. This project was initiated to determine the actual environments that composites must resist in infrastructure applications and detect any composite degradation in such an environment.

17. KEY WORDS	18. DISTRIBUTION STATEMENT
Composites, Infrastructure, Seismic Retrofit	No Restrictions. This document is available through the National Technical Information Service, Springfield, VA 22161

19. SECURITY CLASSIF. (OF THIS REPORT)	20. SECURITY CLASSIF. (OF THIS PAGE)	21. NO. OF PAGES	22. PRICE
Unclassified	Unclassified	57	

AEROSPACE REPORT NO.
ATR-2001(7595)-1

IN-FIELD MONITORING OF THE DURABILITY OF COMPOSITE BONDLINES

Prepared

G. F. Hawkins
Office of Innovative Materials

G. L. Steckel
Materials Science Department

J. P. Nokes
Materials Preocessing & Evaluation Department

J. L. Bauer
Materials Science Department

Approved

W. H. Kao, Director
Materials Science Department
Space Materials Laboratory

D. G. Sutton, Director
Materials Preocessing & Evaluation Department
Space Materials Laboratory

Acknowledgments

The authors would like to thank the following people for their able assistance and advice on this program: Paul Chaffee, Oscar Esquivel, Ben Nelson, George Panos, Jack Shaffer, and Bruce Weiller.

Contents

Figures

Tables

Introduction

It has been demonstrated that composite column jackets can provide confinement, increase ductility, and increase shear capacity in deficient columns. Caltrans sponsored a "Composites for Seismic Retrofit Program" that produced durability data on the sensitivities of the various types of composites to environmental attack. That program addressed the material degradation issues related to environmental, physical, and chemical concerns by using accelerated testing techniques.

The durability study attempted to accelerate the rate of degradation by immersing samples in extreme environments for extended times. However, the performance of composites in actual environments was still largely unknown. This project was initiated to determine the actual environments that composites must resist in infrastructure applications and detect any flaw growth. To that end, for the past two years, an FHWA/Caltrans-sponsored project has been monitoring a number of retrofitted columns at the Yolo Causeway.

The manufacturing method for applying the composite to the columns at the Yolo Causeway involved bonding composite shells to the concrete with adhesive (see Section 1). It was initially assumed that any degradation in this adhesive material could be monitored using infrared (IR) techniques. It was envisioned that optical sensors buried in the bondline would carry the IR information out to detectors on the outside of the column. A study was performed to correlate the adhesive degradation with the IR signature (see Appendix 1). The study concluded that, for the particular adhesive chosen by the contractor, the IR signature is not a good indicator of degradation.

Mechanical Degradation of Exposed Panels. It was decided to monitor the environment surrounding the adhesive and the resulting degradation separately. The degradation was measured from panels of composite material that were mounted on the columns and periodically removed for laboratory analysis. To take full advantage of this opportunity, panels from many different materials were included in this field study. The results are given in Section 2.

Measuring the Bondline Environment. The environment surrounding the adhesive was measured at the columns. The humidity and temperature were measured beneath the composite, at the bondline between the adhesive and the concrete. The humidity and temperature were monitored continuously using a sensor and a data recorder that was downloaded annually. The humidity and temperature results are presented in Section 3.

Growth of Bondline Flaws. The flaw growth will be measured by first detecting the flaws present initially using a thermographic scan of a sufficient number of columns to get a statistically significant sampling of the flaws. Any flaws detected, which Caltrans does not require to be repaired, will be measured and documented using thermography. These flaws will be repeatedly measured throughout the duration of this project. These results are presented in Section 4.

This page intentionally blank.

Section 1. Yolo Causeway Manufacturing Details

In the late winter of 1997, Caltrans initiated a contract (#03379604) with Benco Contracting and Engineering to perform a seismic retrofit on the Interstate 80 Yolo Causeway. The retrofit consisted of constructing new concrete piles at every fourth bent, enclosing existing pile extensions with a composite case, and closing a longitudinal joint at the Tule Canal. The encasement of the concrete columns with composite materials was awarded to the Myers Technologies Business unit of C. C. Myers, Inc. and commenced in the summer of 1998, concluding in October, 1998.

The Yolo Causeway is the portion of I-80, just west of Sacramento that transverses an Estuary at the Tule Canal. It is just over 3 mi. long, a third of which is an earthen berm. The two bridges (22-0044W and 22-0045E) that constitute the remainder of the Causeway consist of 6 lanes of traffic (3EB & 3WB). Figure 1.1 represents the Causeway and illustrates the bridges and earthen berm. Figure 1.2 illustrates the western end of the Causeway, while Figure 1.3 show the columns supporting the deck.

The two outer lanes of the EB and WB original freeway are each supported with 6 15-in.-dia columns (for a total of 12), which were to be retrofitted with composite cases. The newer inner lanes of the freeway were each supported with 3 octagonal columns, which were not encased. A total of more than 3,500 columns were retrofitted. During the winter months, all of the retrofit sections are under water as the estuary is flooded.

The composite encasement used to retrofit the columns was a custom fiberglass cloth impregnated with a polyester resin and precured in the factory. The shells were wound into cylinders matching the column diameter, cured, then slit lengthwise and delivered to the worksite. The shells are then adhesively bonded to the columns using an ambient-temperature cure, two-component resin. A height of 4 ft of each column was retrofitted using four concentric shells per column, with the slit offset on each successive layer.

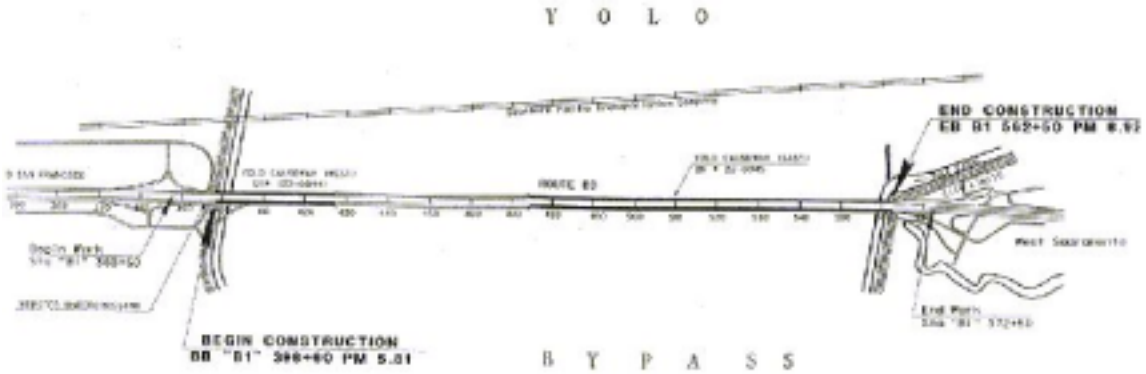

Figure 1.1. Yolo Causeway showing the two bridges at the East and West ends and the Tule Canal at the eastern end of the causeway.

Figure 1.2. Western end of the Yolo Causeway (Bridge 22-0044), showing westbound traffic.

Figure 1.3. View of columns under the Yolo Causeway. A column to the left of center has been retrofitted and still displays the restraining bands. The eight-sided columns in the center did not receive a retrofit.

The fiberglass reinforcement was custom manufactured by Johnson Industries and consisted of unidirectional fiberglass (e-glass) stitched to a polyester vail. The fiberglass fabric was impregnated with an isophthalic polyester resin supplied by McWhorter Technologies and cured at 180°F. A two-component, room-temperature curing polyurethane adhesive from Morton International was used to bond the shells to the column and to each successive overwrapping shell. After all four shells were installed on the column, they were banded in place for a period of 24 h to permit adhesive cure.

The actual retrofit is conducted as follows:

1. The columns are cleaned, usually with a water blast. All foreign material and protubances are removed. Severe depressions are filled with a suitable grout or resin.

2. A two-component urethane adhesive is sprayed on the columns through a meter-mix nozzle. Usually six columns at a time are coated with adhesive. A working life of about 30 min is permitted, depending on the ambient temperature, to fix the adherents (shells) to the adhesive. The first of four preformed shells is fitted around the column. Usually, six columns are so fitted at a time. The precured shells are manually expanded and placed around the column and allowed to snap shut. (See Figure 1.4.)

3. Adhesive is then successively sprayed on the installed shell, and subsequent shells are fitted to the column in the same fashion. The resultant gap in each skin is staggered around the column at 0°, 180°, 270°, and 90°, such that no gaps overlap. (See Figure 1.5.) The apparent gaps in the fitted shells are purposely created. The shells are fabricated with a slightly smaller diameter than the column to permit them to close snugly around the column.

4. Once all four skins are installed on the columns, a release film is wound around the column, and several bailing-wire bands are used to snug the shells tightly together and onto the column. (See Figure 1.6.) The adhesive is then allowed to set for 24 h. Full cure is achieved in 7 days.

Figure 1.4. Workers fit the first skin to a column. They have manually expanded the skin to permit it to encase a column precoated with adhesive. Cured shells and the meter-mix equipment are delivered to the site by the truck in the background.

Figure 1.5. Four shells fitted to a column. The outer shell gap is evident in the right center. The inner skin gap is seen in the upper left.

Figure 1.6. Workers are fitting restraining bans to the retrofit to permit the adhesive to set. Bands will remain on column for 24 h.

5. Two crews of two men each install the shells. The first team sprays the adhesive on a series of columns (usually 3 to 6) and is followed by the second team, which installs the skins. This is repeated until the four skins are installed. Using two two-man teams, four shells can be installed on six columns in 30 min or less if there are no external distractions to these activities.

6. Quality control activities are conducted in the plant as the skins are fabricated and in the field as they are installed.

Section 2. Durability Field Study on Composites Exposed to the Yolo Causeway Environment

2.1 Materials and Field Exposure Procedures

Flat panels of eight different composite systems supplied by six manufacturers are being exposed at the Yolo Causeway in a field study of environmental durability. The different systems and the number of exposure panels for each system are given in Table 2.1. For most composite systems, the panels are from the same material lots that were used for laboratory durability testing conducted by The Aerospace Corporation as part of the Caltrans qualification program for composites for seismic retrofit of bridge columns. Therefore, the material lots are well characterized, and it will be possible to compare the results of the field durability study directly with the results of the laboratory study. The effects of the environmental exposures will be determined from glass-transition temperature measurements, mass measurements, optical microscopy of cross sections, and tensile tests conducted in the fiber direction to determine Young's modulus, ultimate tensile strength, and failure strain.

The test matrix also includes six bonded assemblies (MTA1-MTA6 in Table 2.1). Each bonded assembly consists of two 12 x 6 in. E-glass/Polyester panels bonded together with a polyurethane adhesive. These assemblies are being used for lap shear tests to determine the durability of the adhesive. Glass-transition temperature is also being measured for the adhesive.

The Yolo Causeway was selected for this study because it is in a flood plain in which the composite panels will be submerged in water for several weeks each winter. The laboratory durability study demonstrated that extended moisture exposure is the environment most likely to affect the materials

Table 2.1. List of Composite Materials for Yolo Causeway Field Durability Study

Material Supplier	System Type	Composite System	Panel Numbers
Master Builders, Inc.	Carbon/Epoxy	CF130/MBrace™ Epoxy	T3-2L13A & B, T3-2L21A & B, T3-2L22A & B
Mitsubishi Chemical Co.	Carbon/Epoxy	Replark®30/L700S-LS	M2-2L13A & B, M2-2L21A & B, M2-2L22A & B
Xxsys Technologies, Inc.	Carbon/Epoxy	Akzo/Epon 828	P2C10A & B, P2C12A & B
Fyfe Company	Carbon/Epoxy	SCH 41/Tyfo® S	HF3I1 & 2, HF3K1 & 2, HF3M1 & 2
Fyfe Company	E-glass/Epoxy	SEH 51/Tyfo® S	HF2I1 & 2, HF2K1 & 2, HF2M1 & 2
Fyfe Company	Fiberglass/Epoxy	SEH 51S/Tyfo® S	FG2I1 & 2, FG2J1 & 2
Hardcore Composites	E-glass/Vinyl Ester	E-glass/Vinyl Ester	P32A & B, P34A & B
Myers Technologies, Inc.	E-glass/Polyester	E-glass/Polyester	MT1-MT6
Myers Technologies, Inc.	Adhesive Lap Shear Assemblies	E-glass/Polyester/ MOR-AD-695-28 Adhesive	MTA1-MTA6

in Table 2.1. Therefore, the Yolo Causeway represents one of the most severe environments that the composites will be subjected to in service in California.

Six separate panels are being exposed to the Yolo Causeway environment for six composite systems, and four panels are being exposed for the other three systems. The panels were mounted on octagonal columns under the bridge. The general procedure was to attach all test panels for a given composite system to a single column. Furthermore, two panels were attached, one above the other, on one face of the octagonal column. Therefore, those systems with four test panels were placed on two faces of a column, and those systems with six test panels were placed on three faces of a column. In most cases, the panels were placed on the south, southwest, and west faces of the column. This was done to protect the panels from impact damage from objects carried by wintertime water currents. The top of the upper panel was approximately 60 in. above ground level, and the top of the lower panel was approximately 47 in. above ground level.

In order to attach the panels to the columns, a 0.328-in.-dia hole was drilled through each panel on the centerline approximately 0.6 in. from each end. A polyethylene insert having an outside diameter of 0.312 in. and inside diameter of 0.260 in. was bonded in the hole. A polyurethane sealant was used to bond the inserts into the panels in order to seal the walls of the drilled holes to prevent water from wicking into the panels through exposed fiber ends. Two 0.156-in.-dia holes were drilled into the column for the attachment of each panel using 3/16 x 1.25 in. concrete screws. The composite panel hole inserts had a minimum length of 0.25 in. Therefore, the maximum penetration of the screws into the column did not exceed 1.0 in.

The panels were mounted on a total of nine columns to accommodate the full matrix of materials given in Table 2.1. There are three octagonal columns per bent. The octagonal columns are located in the middle of each bent between six circular columns on the north end and six circular columns on the south end. The circular columns, which support the original eastbound and westbound bridges, required seismic retrofit. The octagonal columns support the central expansion that was added between the original bridges and did not require seismic retrofit. The panels were mounted on all three octagonal columns on each of three bents, Bent Nos. 177, 178, and 179. For each bent, the octagonal columns were identified by their relative positions, north, center, or south.

The panels were mounted under the bridge on October 29, 1998. For those systems having six panels, one panel was removed for property measurements on September 5, 2000, and the second panel was to be removed in early spring 2001 as soon as the location was accessible after the water receded. The third and fourth panels will be removed in the fall of 2002 and spring of 2003, respectively. The fifth and sixth panels will be removed in the spring and fall, respectively, of 2008. The philosophy behind removing the panels for property measurements in the spring and fall is to make comparisons between panels with maximum moisture absorption (spring removal) and those that have dried-out over the hot, dry summer months. Panels are being removed in the spring and fall after approximately 2-, 4-, and 10-year exposures. For those systems with four test panels, removal will be in the spring and fall after approximately 2 or 4 years and after 10 years.

Unfortunately, the water level at the site during the 2000–2001 winter season was lower than normal so that the panels were not submerged. Therefore, the panels were not removed in the spring of 2001.

A new retrieval date for these panels will be scheduled after the panels to be removed in the fall of 2002 and spring of 2003 are evaluated.

The individual panels for each system are listed in Tables 2.2 and 2.3. The glass-fiber-reinforced systems are given in Table 2.2, while the carbon-fiber-reinforced systems are given in Table 2.3. The tables include the specific mounting location for each panel, the scheduled retrieval date, and the initial mass. The retrieval dates for the panels originally scheduled for May−01 retrieval are indicated TBD in Tables 2.2 and 2.3.

Table 2.2. Glass Fiber-Reinforced Composite Panels

Panel No.	Bent No.	Column No.	Side	Position	Retrieval Date	Initial Mass, g
HF-2I1	177	Center	W	Bottom	May-08	323.36
HF-2I2	177	Center	W	Top	Sep-08	325.24
HF-2K1	177	Center	SW	Top	Sep-02	332.11
HF-2K2	177	Center	SW	Bottom	May-03	328.75
HF-2M1	177	Center	S	Top	TBD	331.85
HF-2M2	177	Center	S	Bottom	9/5/00	322.12
FG2I1	178	South	W	Top	May-08	233.84
FG2I2	178	South	W	Bottom	Sep-08	240.48
FG2J1	178	South	S	Top	TBD	237.53
FG2J2	178	South	S	Bottom	9/5/00	226.35
HD-P32A	179	North	W	Bottom	May-08	233.96
HD-P32B	179	North	W	Top	Sep-08	237.09
HD-P34A	179	North	SW	Top	Sep-02	233.59
HD-P34B	179	North	SW	Bottom	May-03	237.61
MT1	179	Center	S	Bottom	9/5/00	NA
MT2	179	Center	S	Top	TBD	NA
MT3	179	Center	SW	Bottom	May-08	NA
MT4	179	Center	SW	Top	Sep-02	NA
MT5	179	Center	W	Bottom	May-03	NA
MT6	179	Center	W	Top	Sep-08	NA
MTA1	179	South	S	Bottom	9/5/00	NA
MTA2	179	South	S	Top	TBD	NA
MTA3	179	South	SW	Bottom	May-08	NA
MTA4	179	South	SW	Top	Sep-02	NA
MTA5	179	South	W	Bottom	May-03	NA
MTA6	179	South	W	Top	Sep-08	NA

Table 2.3. Carbon Fiber-Reinforced Composite Panels

Panel No.	Bent No.	Column No.	Side	Position	Retrieval Date	Initial Mass, g
T3-2L13A	178	Center	SW	Top	Sep-02	76.87
T3-2L13B	178	Center	SW	Bottom	May-03	78.48
T3-2L24A	178	Center	S	Top	TBD	75.37
T3-2L24B	178	Center	S	Bottom	9/5/00	74.72
T3-2L25A	178	Center	W	Top	May-08	72.73
T3-2L25B	178	Center	W	Bottom	Sep-08	68.83
M2-2L13A	177	North	S	Bottom	9/5/00	89.65
M2-2L13B	177	North	S	Top	TBD	84.20
M2-2L21A	177	North	NW	Top	May-08	81.74
M2-2L21B	177	North	W	Top	Sep-08	74.18
M2-2L22A	177	North	SW	Top	Sep-02	82.42
M2-2L22B	177	North	W	Bottom	May-03	81.34
X-P2C10A	178	North	W	Top	Sep-08	178.20
X-P2C10B	178	North	W	Bottom	May-08	186.58
X-P2C12A	178	North	SW	Top	TBD	191.54
X-P2C12B	178	North	SW	Bottom	9/5/00	181.47
HF-3I1	177	South	S	Bottom	9/5/00	155.49
HF-3I2	177	South	S	Top	TBD	148.11
HF-3K1	177	South	SW	Top	Sep-02	155.36
HF-3K2	177	South	SW	Bottom	May-03	153.56
HF-3M1	177	South	W	Top	May-08	160.50
HF-3M2	177	South	W	Bottom	Sep-08	163.69

2.2 Testing Procedures

The effects of the environmental exposures will be determined from matrix glass-transition temperature measurements, T_g, mass measurements, optical microscopy of cross sections, and tensile tests conducted in the fiber direction to determine Young's modulus, ultimate tensile strength, and failure strain. Single-lap shear strength measurements are being made to determine any changes in the bond strength of the adhesive. Pre-exposure and post-exposure photographs are being taken to monitor changes in physical appearance.

Pre-exposure photographs were taken immediately after mounting the panels on the columns. Additional field photographs were taken in September 1999 after one year of exposure and will be repeated periodically throughout the 10-year exposure period. After the panels are removed from the columns and returned to the laboratory, they will be cleaned in tap water using a soft brush. After cleaning, additional photographs will be taken to document any changes in physical appearance.

As noted above, a polyurethane sealant was used to bond the mounting inserts into the panels in order to seal the walls of the drilled holes to prevent water from wicking into the panels through exposed fiber ends. The sealant was also used to prevent wicking along any machined or saw-cut panel edges. Pre-exposure mass measurements were made after the polyurethane sealant cured at ambient

temperature. Post-exposure mass measurements are being made after the panels are cleaned and dried.

Following mass measurements, the panels are being sectioned using a water-cooled diamond cut-off wheel to give a 10 x 6 in. (25.4 x 15.2 cm) area for the preparation of five tensile samples and a 0.5-in. (1.3 cm) wide strip for one T_g sample. The tensile and T_g samples are cut out with the sample length parallel to the primary fiber direction.

Uniaxial tensile tests are performed using straight-sided, tabbed samples following sample preparation and test procedures specified in ASTM D 3039.[2-1] G10 fiberglass/epoxy grip tabs 0.063 in. (0.16 cm) thick and 2.0 in. (5.1 cm) long with a 7° taper are bonded across both ends on each side of the panel section for tensile samples. The grip tabs are bonded using Hysol EA 9394 adhesive that is cured at ambient temperature. The adhesive is allowed to cure for a minimum of two days before five 0.75-in. (1.9-cm) wide tensile samples are cut from the tabbed panel section using a water-cooled diamond cut-off wheel. The grip tabs are allowed to cure a minimum of five days prior to tensile testing. Tensile testing is performed using an Instron Universal Testing Machine having wedge grips. Strain is measured throughout the test using a 2.0-in. (5.1-cm) gage length, clip-on extensometer. Samples are loaded to failure at a constant crosshead rate of 0.2 in./min (0.51 cm/min), giving an approximate strain rate of 0.0017 s^{-1}. Load and strain are recorded with a strip chart recorder and a computer data acquisition system. Young's modulus is calculated by a least-squares analysis of the stress-strain curve over the strain range from 0 to 0.50%.

T_g of the composite matrix is being determined using a Rheometrics Dynamic Mechanical Analyzer (DMA). The Rheometrics DMA subjects a 2.0 x 0.5 in. (5.1 x 1.3 cm) sample to cyclic torsional deformations and quantifies the material response by measuring the shear modulus, G', the shear loss modulus, G", and the lag angle between the applied stress and resulting strain, tan δ, as functions of temperature. Plots of any of these three parameters versus temperature can be used to determine T_g. In this program, the G" curve is used because it usually gives a sharp peak at the transition, making it easier to determine T_g than for the tan δ or G' curves.

Differential scanning calorimetry (DSC) using a TA Instruments Model No. 2910 DSC was used to measure T_g for the adhesive in the Myers Technologies, Inc. bonded assemblies. Approximately 5 mg of adhesive was scraped from the bond line of the bonded assemblies for analysis. Heat flow was measured during heating at 9°F/min (5°C/min) over the temperature of –50 to 212°F (–60 to 100°C). T_g was determined from plots of heat flow versus temperature following standard procedures.[2-2]

For the preparation of single lap shear samples, the Myers Technologies, Inc. bonded assemblies are cut parallel to the fiber direction with the diamond cut-off wheel into five 6 x 1.0 in. (15 x 2.5 cm) strips. The two composite adherrends are cut along locations A and B as shown in Figure 2.1 to form the lap shear area. Thus, the lap shear samples have a 0.5 in. (1.3 cm) long single-lap configuration. It is pointed out in ASTM D 4896, "Standard Guide for Use of Adhesive-Bonded Single Lap-Joint Specimen Test Results,[2-3]" that the true shear stress of an adhesive joint can not be easily determined using single-lap specimens. The major problem is that the bending moment inherent in single-lap specimens induces tensile stresses normal to the plane of the bondline at the ends of the overlap and a nonuniform shear stress distribution in the adhesive. Thus, the measured shear stress at failure is

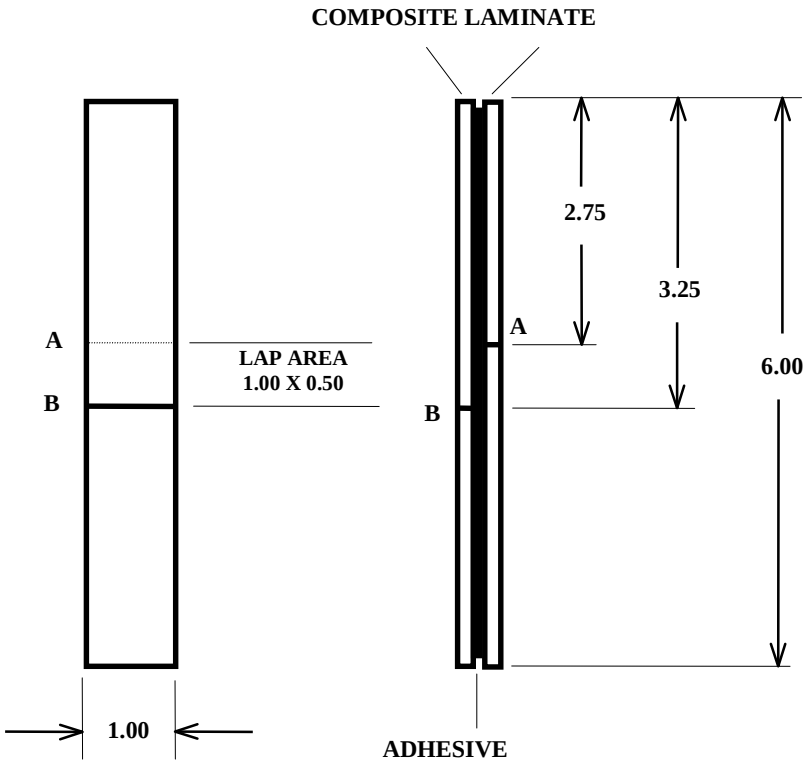

Figure 2.1. Drawing for preparation of single lap shear samples from bonded composite panel assemblies.

lower than the true shear strength of the joint. Therefore, the steel fixture shown in Figure 2.2 is used to reduce bending of the composite adherrends. The overlap area of the sample is centered within the 2 in. (5.1 cm) long fixture so that bending stresses on the adherrends are resisted by the steel plates at positions approximately 0.75 in. (1.9 cm) outside the overlap area. During installation, the screws are tightened only to the point at which the clamping force is sufficient to prevent the steel fixture from sliding down the sample under the force of gravity. Thus, high compressive normal stresses on the adhesive bondline are avoided. The fixture eliminates failures due to peeling stresses. The lap shear testing is performed in an Instron Universal Testing Machine at a crosshead rate of 0.1 in/min (0.25 cm/min).

2.3 Preliminary Results

Comparative photographs taken immediately after mounting the panels on the columns in October 1998 and after the first year of exposure in September 1999 are shown in Figures 2.2 through 2.6 for the carbon-fiber-reinforced systems and in Figures 2.7 through 2.11 for the glass-fiber-reinforced systems. The effects of wintertime flooding and subsequent drying are evident by cracking of the soil around the columns in the one-year photographs. All of the panels were obviously soiled from the

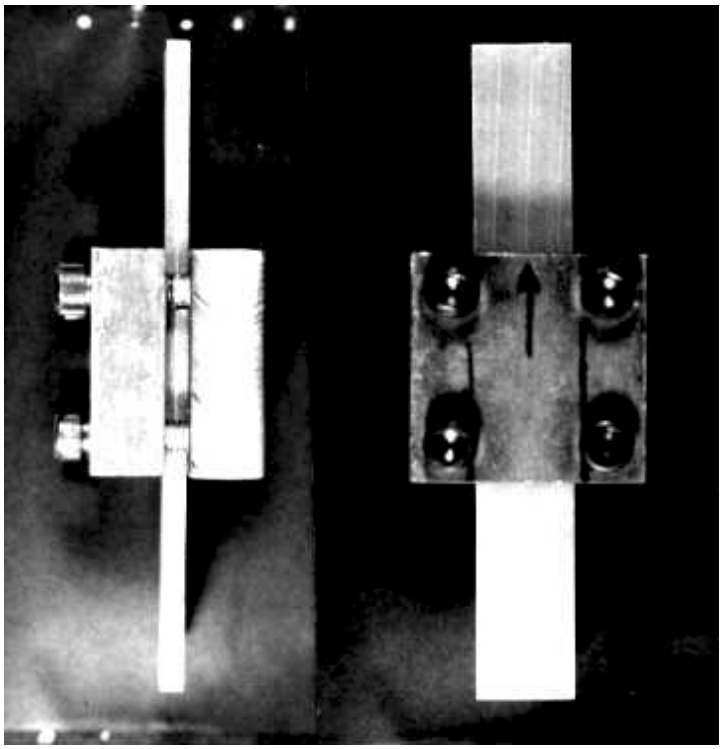

Figure 2.2. Anti-bending fixture for single lap shear testing.

Figure 2.3. Photographs of Fyfe Co. SCH 41/Tyfo S carbon/epoxy panels taken at beginning (left) and after 1-yr field exposure.

Figure 2.4. Photographs of Mitsubishi Chemical Corp. Replark 30/L700S-LS carbon/epoxy panels taken at beginning (left) and after 1-yr field exposure. Panel No. M2-2L1A was mounted on northwest side of the column and is not shown in photographs.

Figure 2.5. Photographs of Master Builders, Inc. CF130/MBrace™ Epoxy Carbon/Epoxy panels taken at beginning (left) and after 1-yr field exposure.

Figure 2.6. Photographs of Xxsys Technologies, Inc. Akzo/Epon 828 Carbon/Epoxy panels taken at beginning (left) and after 1-yr field exposure.

Figure 2.7. Photographs of Fyfe Co. SEH 51/Tyfo S E-glass/Epoxy panels taken at beginning (left) and after 1-yr field exposure.

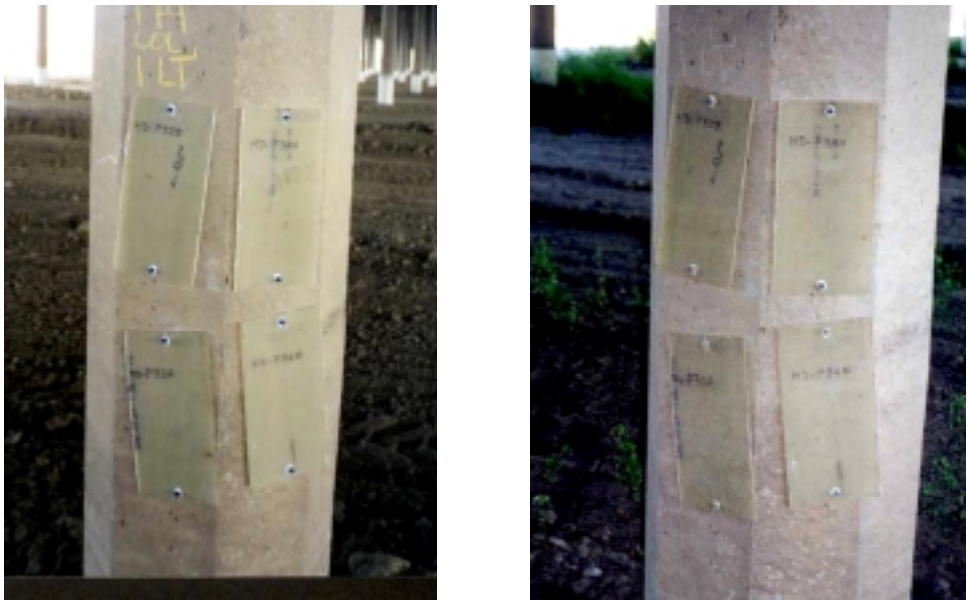

Figure 2.8. Photographs of Hardcore Composites E-glass/Vinyl Ester panels taken at beginning (left) and after 1-yr field exposure.

Figure 2.9. Photographs of Fyfe Co. SEH 51S/Tyfo® S Fiberglass/Epoxy panels taken at beginning (left and middle) and after 1-yr field exposure.

Figure 2.10. Photographs of Myers Technologies, Inc. E-glass/Polyester panels taken at beginning (left) and after 1-yr field exposure.

Figure 2.11 Photographs of Myers Technologies, Inc. E-glass/Polyester/MOR-AD-695-28 Adhesive bonded panels taken at beginning (left) and after 1-yr field exposure.

one-year exposure. Sample identification numbers were obscured or removed from several panels, particularly the E-glass/polyester panels fabricated by Myers Technologies, Inc. However, there was no evidence of physical damage to any of the composite panels following the first year of exposure.

The first panel was removed from the columns for all composite systems, except the Hardcore Composites E-glass/vinyl ester system on September 5, 2000. The specific panels removed are identified in Tables 2.2 and 2.3. At that time, all of the panels were inspected and continued to show no evidence of physical damage.

The retrieved panels were returned to the laboratory for cleaning, further inspection, and mechanical and physical property measurements. Visual inspection following brush cleaning in tap water gave no indications of any changes in physical appearance for any of the composite systems.

The tensile properties, matrix glass-transition temperature, and moisture absorption for the carbon-fiber-reinforced composites are given in Table 2.4. The data for the two-year Yolo Causeway exposure are compared to average values for four control (baseline) panels and the results of a 1.1-year (10,000-h) pH 9.5 alkali solution exposure. The control and alkali exposure data are from the laboratory qualification test program. The most severe exposures in the qualification program were 1.1 year in 100% humidity at 100°F (38°C), 1.1 year in salt water at room temperature, and 1.1 year in the alkali solution at room temperature. None of these exposures had any significant effects on the tensile properties on any of the carbon/epoxy composite systems. However, the salt water and alkali

Table 2.4. Mechanical and Physical Properties of Carbon Fiber-Reinforced Composite Panels

Composite System Exposure Conditions	Young's Modulus, msi	Tensile Strength, ksi	Failure Strain, %	Glass Transition Temp, °F (°C)	Moisture Absorption, %
Fyfe Company SCH 41/Tyfo® S Epoxy					
Control	9.15 ± 0.27	136 ± 9	1.44 ± 0.11	154 (68)	
2 yr at Yolo	9.78 ± 0.39	144 ± 7	1.48 ± 0.12	154 (68)	0.14
1.1 yr in Alkali Solution	9.50 ± 0.28	144 ± 6	1.45 ± 0.06	147 (64)	1.28
Master Builders, Inc. CF130 (T700)/MBrace™ Epoxy					
Control	32.8 ± 1.8	636 ± 27	1.75 ± 0.09	156 (69)	
2 yr at Yolo	33.7 ± 0.7	536 ± 29	1.50 ± 0.08	153 (67)	0.24
1.1 yr in Alkali Solution	33.1 ± 1.5	615 ± 39	1.70 ± 0.12	144 (62)	1.31
Mitsubishi Chemical Corp. Replark® 30 (T700)/L700S-LS Epoxy					
Control	33.6 ± 1.2	605 ± 35	1.65 ± 0.10	147 (64)	
2 yr at Yolo	33.3 ± 1.2	599 ± 52	1.67 ± 0.12	147 (64)	No Data
1.1 yr in Alkali Solution	32.7 ± 0.7	595 ± 58	1.64 ± 0.11	142 (61)	1.78
Xxsys Technologies, Inc. Akzo/Epon 828 Epoxy					
Control	28.5 ± 0.9	356 ± 31	1.24 ± 0.11	147 (64)	
2 yr at Yolo	30.1 ± 0.6	375 ± 10	1.24 ± 0.05	147 (64)	0.04
1.1 yr in Alkali Solution	26.3 ± 0.6	381 ± 11	1.42 ± 0.04	126 (52)	0.96

exposures tended to have the most significant effect on T_g. Therefore, the alkali exposure was selected as being representative of the most severe exposures from the laboratory testing. The tensile properties shown in the table for the Yolo and alkali exposures are average values for five samples, while those for the control are average values for 20 samples. Standard deviations are also given. The T_g values are the averages for four samples from four different panels for the control condition and single samples for the Yolo and alkali exposures. It is assumed that any changes in mass resulting from the exposure are due to moisture absorption or moisture dry-out.

It should be noted that the tensile properties for the Master Builders, Inc., Mitsubishi Chemical Corp., and Xxsys Technologies, Inc. composites were calculated based on the know fiber area of the tensile samples. Therefore, the tensile properties are representative of the fiber properties in the fabricated composites. This is the standard method of calculating tensile properties used by Master Builders, Inc. and Mitsubishi Chemical Corp. Master Builders and Mitsubishi both use high-strength T700 carbon fibers. Therefore, it is not surprising that the Master Builders, Inc. CF130/MBrace™ epoxy and Mitsubishi Chemical Corp. Replark® 30/L700S-LS systems had similar tensile properties. Xxsys Technologies, Inc. used a slightly lower modulus and significantly lower strength fiber; hence the lower properties for their system. The tensile properties for the Fyfe Co. SCH 41/Tyfo® S system are calculated using a standard thickness of 0.041 in./ply, which is similar to the actual per ply thickness of the composite. Thus, the SCH 41/Tyfo S properties are essentially based on the composite area and are, therefore, much lower than those for the other three carbon fiber systems, which were based on the fiber area only.

As the data in Table 2.4 demonstrate, the 1.1-year exposure in the alkali solution had no effects on the tensile properties of the carbon-fiber-reinforced systems. And as noted above, none of the laboratory exposures had a significant effect on the tensile properties of these systems. Therefore, no change in tensile properties was anticipated from the two-year Yolo Causeway exposure. The anticipated result was obtained for the Fyfe Co., Mitsubishi Chemical Corp., and Xxsys Technologies, Inc. systems, but the Master Builders, Inc. system had a 15% reduction in tensile strength and failure strain relative to the control properties. However, we believe that this is an anomalous effect. The two-ply CF130/MBrace epoxy panel exposed at Yolo Causeway for two years was 0.059 in. thick. The 18 panels tested in the laboratory environmental durability program were within the 0.038–0.048 in. thickness range. The higher thickness of the Yolo panel is indicative of a higher epoxy resin content or a significantly higher void volume. These differences may have caused the lower tensile strength. Previous studies have shown that this system is susceptible to reduced tensile strength from high porosity.[2.4] Optical microscopy of this panel is being conducted to determine the resin and porosity content.

The data in Table 2.4 show that the two-year Yolo Causeway exposure had no effect on T_g for the epoxy matrix of any of the four systems. The most frequent cause of reductions in T_g from environmental exposures is from moisture absorption, as demonstrated by the 1.1-year alkali exposure. In the present case, the Yolo Causeway panels were retrieved in the fall after being exposed to hot, dry weather throughout the summer. Thus, the moisture content was very low. In the future, panels will be removed in the spring immediately after the water level subsides. These panels should have the maximum absorbed moisture content, and thus the lowest T_g for the Yolo Causeway site.

The tensile properties, matrix glass-transition temperature, and moisture absorption for the glass-fiber-reinforced composites are given in Table 2.5. Glass fibers are susceptible to strength degradation in moist environments, which was demonstrated in the laboratory durability testing. Strength degradation was particularly evident from the 100% humidity exposure at 100°F (38°C), especially for the SEH 51/Tyfo S and SEH 51S/Tyfo S systems. Therefore, the data in Table 2.5 includes 0.1-, 0.3-, and 1.1-year data for the alkali solution and humidity exposures from the laboratory qualification test program for comparison with results for the two-year Yolo Causeway exposure.

Table 2.5. Mechanical and Physical Properties of Glass-Fiber-Reinforced Composite Panels

Composite System Exposure Conditions	Young's Modulus, msi	Tensile Strength, ksi	Failure Strain, %	Glass Transition Temp, °F (°C)	Moisture Absorption, %
Fyfe Company SEH 51/Tyfo® S					
Control	3.96 ± 0.13	80.5 ± 5.1	2.10 ± 0.18	151 (66)	
2 yr at Yolo	4.13 ± 0.14	79.9 ± 2.8	2.03 ± 0.03	154 (68)	0.15
0.1 yr in Alkali Solution	3.85 ± 0.03	83.2 ± 2.8	2.25 ± 0.11	149 (65)	0.36
0.3 yr in Alkali Solution	4.00 ± 0.13	80.8 ± 4.1	2.11 ± 0.11	142 (61)	0.53
1.1 yr in Alkali Solution	3.88 ± 0.06	62.4 ± 2.5	1.63 ± 0.08	147 (64)	0.88
0.1 yr in Humidity/100°F	4.04 ± 0.13	71.6 ± 2.8	1.82 ± 0.08	162 (72)	0.56
0.3 yr in Humidity/100°F	3.94 ± 0.10	67.9 ± 1.9	1.77 ± 0.05	163 (73)	0.82
1.1 yr in Humidity/100°F	3.93 ± 0.18	51.4 ± 2.1	1.31 ± 0.08	163 (73)	1.09
Fyfe Company SEH 51S/Tyfo® S					
Control	5.03 ± 0.12	111 ± 3	2.56 ± 0.13	165 (74)	
2 yr at Yolo	5.15 ± 0.06	110 ± 1	2.45 ± 0.08	162 (72)	0.11
0.1 yr in Alkali Solution	5.08 ± 0.01	104 ± 4	2.28 ± 0.09	153 (67)	0.36
0.3 yr in Alkali Solution	4.85 ± 0.15	105 ± 3	2.46 ± 0.13	154 (68)	0.65
1.1 yr in Alkali Solution	4.90 ± 0.17	94 ± 3	2.06 ± 0.08	149 (65)	1.11
0.1 yr in Humidity/100°F	4.79 ± 0.15	103 ± 4	2.41 ± 0.18	165 (74)	0.70
0.3 yr in Humidity/100°F	4.74 ± 0.11	83 ± 5	1.83 ± 0.10	172 (78)	1.02
1.1 yr in Humidity/100°F	4.66 ± 0.07	75 ± 5	1.68 ± 0.12	162 (72)	1.23
Myers Technologies, Inc. E-Glass/Polyester					
Control	5.29 ± 0.21	93 ± 12	1.83 ± 0.19	246 (119)	
2 yr at Yolo	5.84 ± 0.18	96 ± 5	1.72 ± 0.05	241 (116)	No Data
0.1 yr in Alkali Solution	5.50 ± 0.12	102 ± 2	1.99 ± 0.03	232 (111)	0.17
0.3 yr in Alkali Solution	5.42 ± 0.09	93 ± 3	1.76 ± 0.08	192 (89)	0.26
1.1 yr in Alkali Solution	5.20 ± 0.11	82 ± 4	1.67 ± 0.10	190 (88)	0.30
0.1 yr in Humidity/100°F	5.65 ± 0.28	92 ± 9	1.75 ± 0.18	244 (118)	0.26
0.3 yr in Humidity/100°F	5.54 ± 0.09	101 ± 2	1.96 ± 0.08	232 (111)	0.28
1.1 yr in Humidity/100°F	5.45 ± 0.23	86 ± 7	1.61 ± 0.08	235 (113)	0.20

The tensile properties for the SEH 51/Tyfo S and SEH 51S/Tyfo S systems are calculated using a standard thickness of 0.040 in./ply, which is similar to the actual per ply thickness of the composite. The tensile properties for the Myers Technologies, Inc. E-glass/Polyester system are calculated using the actual sample area. Thus, the three glass-fiber-reinforced systems have similar tensile properties. The Fyfe Co. composites are reinforced by an unbalanced fabric, while the Myers Technologies, Inc. system is primarily reinforced by unidirectional fibers. As a result, the Fyfe Co. systems have lower Young's moduli and higher failure strains than the Myers Technologies, Inc. composite.

The primary difference between the SEH 51/Tyfo S and SEH 51S/Tyfo S systems is the glass fibers. The SEH 51 fabric has E-glass fibers, while the SEH 51S fabric has Owens Corning's Advantex fiber. The Advantex fiber is a boron-free fiber developed by Owens Corning as a replacement for E-glass fibers. The mechanical properties of Advantex fibers are similar to those for E-glass fibers. In the present case, the SEH 51S/Tyfo S composite was 30% stronger than the SEH 51/Tyfo S composite. However, this is misleading since the SEH 51/Tyfo S composite tested in this program had lower tensile strength than typical SEH 51/Tyfo S composite lots.

The SEH 51/Tyfo S and SEH 51S/Tyfo S systems behaved similarly in the laboratory study. Neither system was significantly affected by the 0.1- or 0.3-year alkali solution exposures, but the tensile strength of both systems was degraded by over 15% following the 1.1-year alkali exposure. In the humidity exposure at 100°F (38°C), both systems had a progressive decrease in tensile strength with exposure time. After 1.1 year in the humidity chamber, the tensile strength of both systems was degraded by over 30%. The Myers Technologies, Inc. system was also degraded following the 1.1-year exposures in the humidity chamber and alkali solution. However, the degradation was much smaller, around 10–15%.

The results for the 2-year Yolo Causeway exposure were favorable since none of the three glass-fiber-reinforced systems showed any strength degradation. The total time that the panels were submerged under water was approximately two months, from late February to late March, 1999 and 2000. During those periods, the column temperature was approximately 50°F (10°C). Therefore, the total time under water at the Yolo Causeway (≈0.15 year) was less than the 0.3-year laboratory exposure to the alkali solution. Furthermore, the temperature was much lower, which decreases the degradation rate. Therefore, the fact that none of the glass-fiber-reinforced systems showed any degradation after the two-year Yolo exposure is consistent with the laboratory results.

None of the glass-fiber-reinforced systems showed any significant changes in the matrix T_g after the two-year Yolo exposure. As for the carbon-fiber-reinforced systems, this observation is consistent with the fact that there was very little moisture absorption at the time that the panels were retrieved.

The lap shear strength and adhesive T_g results for the Myers Technologies, Inc. E-glass/polyester panels bonded together with MOR-AD-695-28 polyurethane adhesive are presented in Table 2.6. Myers Technologies, Inc. supplied seven bonded assemblies for the Yolo Causeway field durability study. Six bonded assemblies were mounted on the columns, and one was maintained in The Aerospace Corporation Composites Laboratory as a control panel. The bonded assemblies were fabricated in September 1998 at the time that Myers Technologies, Inc. was completing the Yolo Causeway

Table 2.6. Lap Shear Strength of Polyurethane Adhesive Bonded Assemblies

Adhesive Assembly Set Exposure Conditions	Lap Shear Strength, psi	Failure Mode	Glass Transition Temperature, °F (°C)
Yolo Causeway Field Durability Study			
1 Control Assembly	2060 ± 140	Adhesive	72 (22)
2 yr at Yolo	780 ± 100	Cohesive	72 (22)
Yolo Causeway Seismic Retrofit Project Adhesive Acceptance Testing			
Assembly No. A8B16	1730 ± 360	Mixed Mode	77 (25)
Assembly No. A8B18	1110 ± 630	Adhesive	
Assembly No. A13B15	1370 ± 90	Cohesive	
Assembly No. A6B8	1690 ± 180	Cohesive	
Assembly No. A12B14	1200 ± 140	Cohesive	
Assembly No. A14B14	1730 ± 130	Mixed Mode	
Limited Laboratory Durability Study			
1 Control Assembly	1190 ± 140	Adhesive	50 (10)
0.36 yr in Humidity/100°F	1460 ± 50	Adhesive	55 (13)
2.1 yr in Humidity/100°F	900 ± 40	Cohesive	50 (10)

seismic retrofit project. The bonded assemblies for the field durability study were fabricated following the same procedures that were used for preparing test panels for acceptance testing of the adhesive lots used in retrofit project. The Aerospace Corporation performed lap shear strength acceptance testing for six adhesive lots. The results from these tests are also presented in the table to provide additional baseline data.

Unfortunately, Myers Technologies, Inc. made a significant change in their fabrication process that invalidated the laboratory environmental durability test results. Initially, the E-glass/polyester composites were fabricated using a release film, which gave the composites a very smooth surface. During environmental durability qualification testing, it was determined that the lap shear strength was only around 200 psi with the smooth composite surfaces. Myers Technologies, Inc. subsequently incorporated a woven-peel ply into the composite fabrication process. The woven-peel ply provides a very rough surface, which increased the lap shear strength to over 1000 psi. Shortly after incorporating the woven-peel ply into their process, Myers Technologies, Inc. provided two bonded assemblies to Aerospace for evaluation. One of these assemblies (No. BP/10-1) was sectioned into four 6 x 4 in. sub-assemblies with one used for baseline testing and the other three placed into the humidity chamber on July 15, 1998. Part No. BP/10-1A was removed for testing after approximately 3,150 h (0.36 yr), and a Part No. BP/10-1B was removed for testing along with the 2-yr Yolo Causeway panel. Part No. BP/10-1B had been in the humidity chamber for 18,140 h (2.1 yr). Five lap shear samples 0.75 in. wide were tested for each sub-assembly. The humidity exposure for Part No. BP/10-1C is continuing.

The results for the field durability study show a 60% reduction in lap shear strength for the 2-yr exposure relative to the control assembly. In addition, the control samples exhibited an adhesive failure mode, while the 2-yr exposure samples exhibited cohesive failures within the adhesive layer. These

results suggest a large reduction in the shear strength of the MOR-AD-695-28 adhesive from the 2-yr Yolo Causeway exposure. However, it is surprising that there was no change in T_g associated with this apparent degradation.

The lap shear strength data show a high degree of variability between the six Yolo Causeway seismic retrofit acceptance assemblies. Furthermore, some of these baseline assemblies failed predominantly in an adhesive mode, while others failed in a cohesive mode or a mixture of the two modes. These six panel assemblies were bonded using different lots of adhesive, while the field durability study panels were bonded together using a single lot of adhesive. Therefore, less scatter between assemblies would be expected for the field durability than for the acceptance tests. Nevertheless, the large scatter band for the acceptance tests does indicate that it can not be assumed that the differences between the 2-yr Yolo exposure samples and the control samples are due solely to environmental effects. Additional evaluation of the adhesive layer for the field durability samples is needed.

One possible cause of variability is porosity within the adhesive layer. Optical microscopy of core samples from Yolo Causeway casings and one of the acceptance bonded assemblies have shown that the adhesive layer typically has porosity.[2-5] It is conceivable that variations in the porosity content could cause large changes in the lap shear strength and failure mode. Optical microscopy will be performed on the field durability panels and the acceptance panels to address this issue.

The results for the laboratory humidity exposure were also inconclusive. In this case, the results were clouded by the fact that the glass-transition temperature of the adhesive in the bonded assembly was much lower than typical values of >70°F (21°C). Thus, the adhesive did not reach its normal cure state. This could be due to any of several causes, such as improper mixing, out-of-date material, or exposure to low temperatures during cure. After exposure to 100% humidity at 100°F (38°C) for 0.36 yr, the lap shear strength increased by approximately 20%, and T_g increased from 50 to 55°F (10 to 13°C). These effects were probably due to additional cure of the adhesive due to the elevated temperature in the humidity chamber. However, after exposure to 100% humidity at 100°F (38°C) for 2.1 yr, the lap shear strength decreased from 1460 to 900 psi (38% reduction) and T_g decreased back to its original value. In addition, the failure mode reverted from adhesive failures to cohesive failures. Thus, the long-term humidity exposure caused adhesive degradation, but the relevance of the data is uncertain due to the low initial T_g of the adhesive.

The current results cause concern regarding the environmental durability of adhesive bonds for the Myers Technologies system. However, additional data from the field durability bonded assemblies scheduled for retrieval in September 2002 and May 2003 are needed to hopefully resolve inconsistencies in the current data. In the meantime, optical microscopy will be performed on all the bonded assemblies in Table 2.6 to establish any influence of adhesive porosity on the experimental results. Additional laboratory durability data will be obtained by exposing untested lap shear samples from the acceptance panels to room-temperature water.

Continuation of the field durability study is being funded by a separate Caltrans program.

2.4 References for Sec. 2

2-1."Standard Test Method for Tensile Properties of Polymer Matrix Composite Materials," ASTM D 3039, *Annual Book of ASTM Standards*, Vol. 15.03, pp. 114-123 (1995).

2-2."Standard Test Method for Transition Temperatures of Polymers by Thermal Analysis," ASTM D 3418, *Annual Book of ASTM Standards*, Vol. 15.03, pp. 114-123 (1995).

2-3."Standard Guide for Use of Adhesive-Bonded Single Lap-Joint Specimen Test Results," ASTM D 4896, *Annual Book of ASTM Standards*, Vol. 15.06, pp. 401-405 (1997).

2-4.H. S. Kliger and G. L. Steckel, "FORCA Tow Sheet Material Qualification: Practical Aspects of Field and Laboratory Testing," *SAMPE Journal*, Vol. 33, No. 4, pp. 68-71 (July/August 1997).

2-5.G. L. Steckel, "Evaluation of Composite Casing Core Samples from the Yolo Causeway Seismic Retrofit Project," The Aerospace Corporation Report No. ATR-01(7796)-1 (2001).

Section 3. Continuous Temperature and Humidity Measurements

3.1 Introduction and Background

Adhesives need to perform for many years. Laboratories attempt accelerated tests to predict the useful lifetime of materials with tests performed in a reasonable time. The accelerated test methods involve exposing the materials to high temperatures and humidity. Mechanical tests are performed on these samples and the results are compared to control samples that have been kept in a benign environment. To extrapolate the test results and predict the material's lifetime, the conditions of the actual environment need to be determined. In addition, actual field condition monitoring verifies that the accelerated methodology was not benign or too severe.

The humidity, temperature, and pH were measured underneath the composite, at the bondline between the adhesive and the concrete. The humidity and temperature were monitored hourly using a sensor and a data recorder that was downloaded every year. The pH was only measured yearly because it does not exhibit large day-to-day variations.

3.2 Temperature/Relative Humidity Sensors and Data Acquisition

Onset Computer Corporation of Bourne MA manufactured the sensors chosen to measure the temperature and relative humidity (HOBO Pro series). These battery-powered sensors can store up to 65,000 data points over a period of three years. The sensors were programmed to acquire temperature and humidity data every hour. They have the specifications listed below.

3.2.1 Sensor Specifications

3.2.1.1 Temperature

Range –22°F to 158°F
Accuracy: 0.7°F
Resolution: 0.5°F
Response Time: <30 min

3.2.1.2 Relative Humidity

Range: 0% to 100% RH
Accuracy: 3%
Drift: 1% per year
Response Time: <30 min in still air.

Note: Relative Humidity is the ratio of the existing amount of water vapor in the air at a given temperature to the maximum amount that the air can hold at that temperature.

The response of the RH sensor used in these loggers varies not only with RH but also with temperature. To display properly compensated RH values, the software takes the temperature data logged simultaneously with the uncompensated RH data and determines an RH adjustment factor. At 70°F, this adjustment factor is zero. At temperatures other than 70°F, the adjustment factor is added or subtracted to the uncompensated RH reading, dependening on whether the temperature is above or below 70°F. The result is the final compensated RH value.

3.3 Sensor Mounting

The sensors were mounted in sections of 3-1/2-in.-dia PVC pipe (See Figure 3.1). The front of the sensor was in a small volume of air that would be exposed to the concrete of the column. The back of the sensor was mounted to a plate to make the data output port accessible from the rear. The back portion of the PVC pipe was sealed with a removable watertight cover.

A 1-in.-dia hole was drilled in the overwrap to expose the underlying concrete. The PVC pipe containing the sensor was bonded to the composite such that the sensor area was directly over the hole in the composite.

In this manner, the sensor measures the temperature and humidity of the air enclosed by the PVC pipe. This volume of air is directly exposed to the concrete. As the moisture in the concrete changes, the relative humidity in the enclosed volume of air changes correspondingly with a small time lag. The humidity and temperature data is taken each hour and stored in the sensor's memory. The data is downloaded from the memory once a year by removing the back cover and connecting a computer to the data output port.

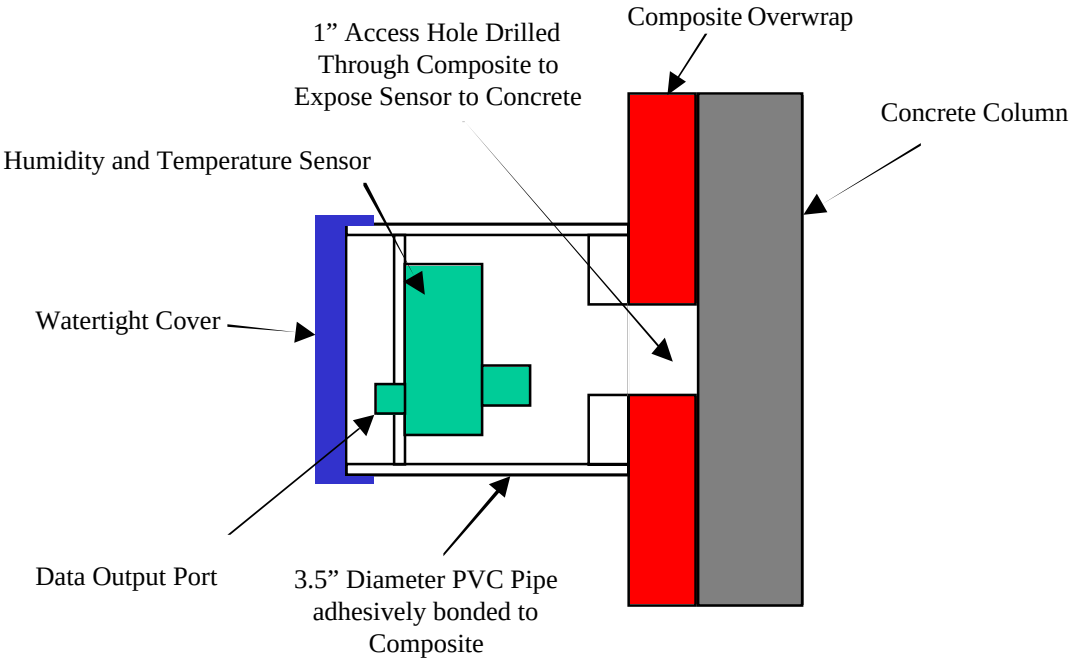

Figure 3.1. Schematic diagram of the technique for mounting the humidity/temperature sensor on the composite overwrapped column.

3.4 Results and Discussion

Hourly data of the relative humidity and temperature taken from the bondline area of the Yolo columns is presented in figures 3.2–3.7. The data was taken over a period of almost two years.

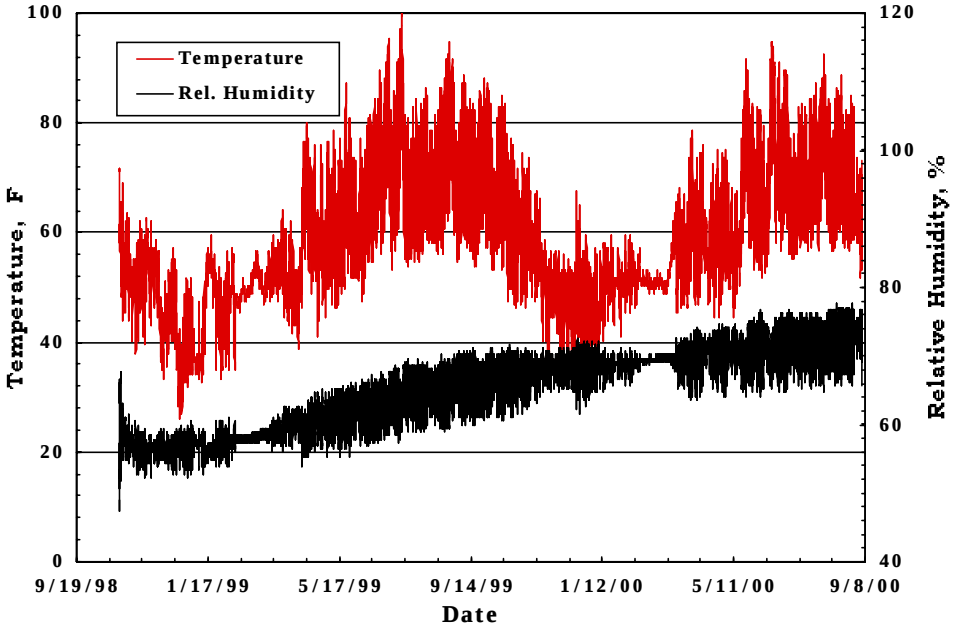

Figure 3.2. Temperature and relative humidity data taken once per hour on Column 7 of Bent 177. The sensors is located at the top on the overwrap casing.

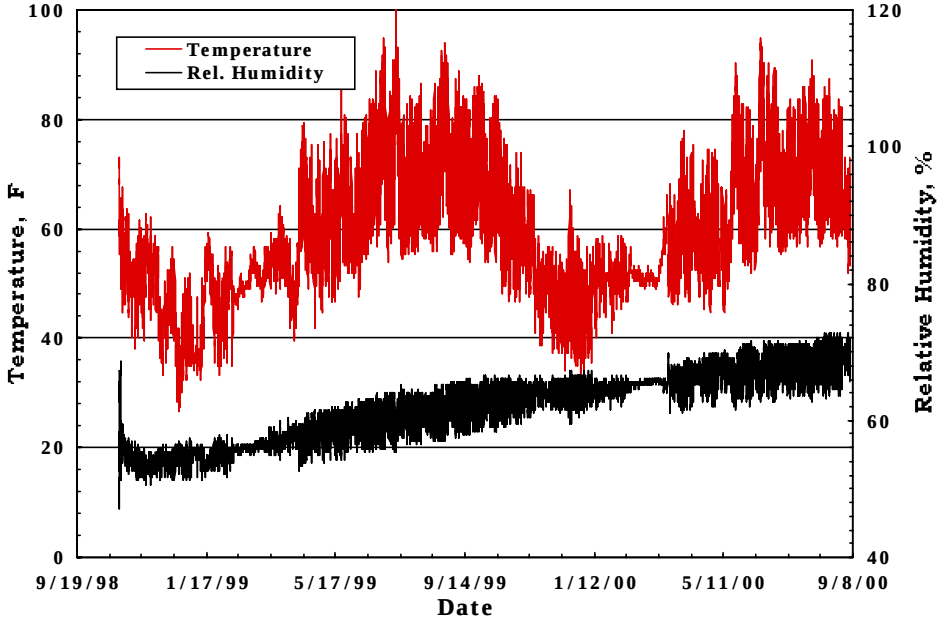

Figure 3.3. Temperature and relative humidity data taken once per hour on Column 7 of Bent 177. The sensors is located at the middle on the overwrap casing.

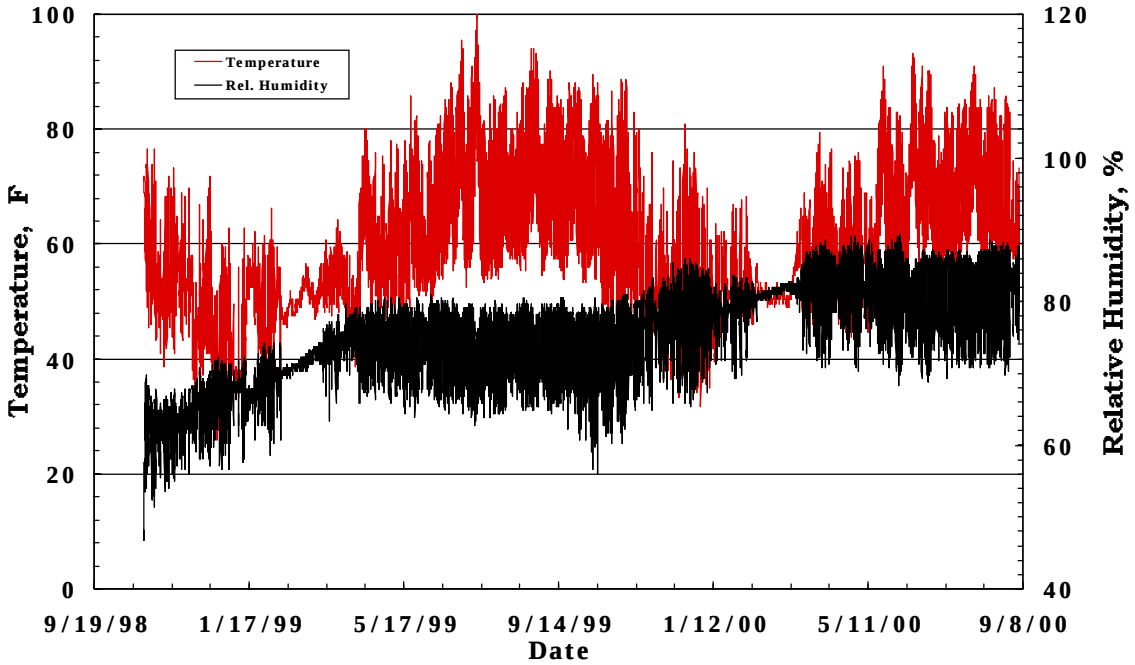

Figure 3.4. Temperature and relative humidity data taken once per hour on Column 3 of Bent 178. The sensors is located at the middle on the overwrap casing.

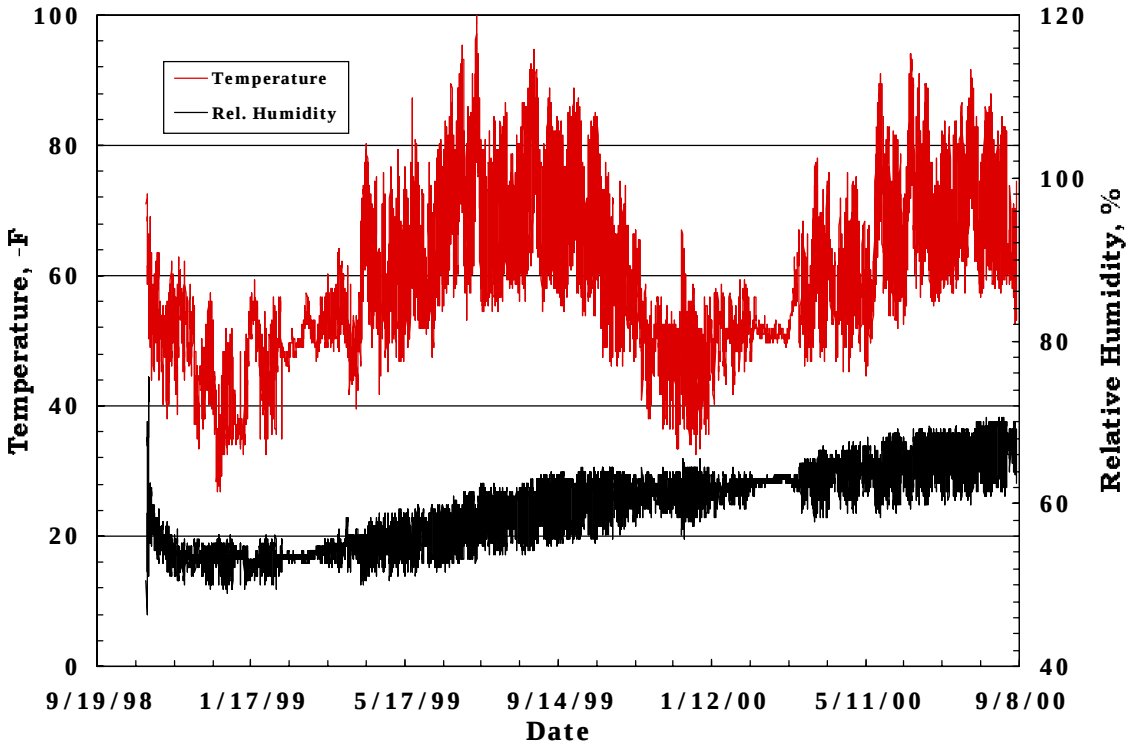

Figure 3.5. Temperature and relative humidity data taken once per hour on Column 8 of Bent 178. The sensors is located at the top on the overwrap casing.

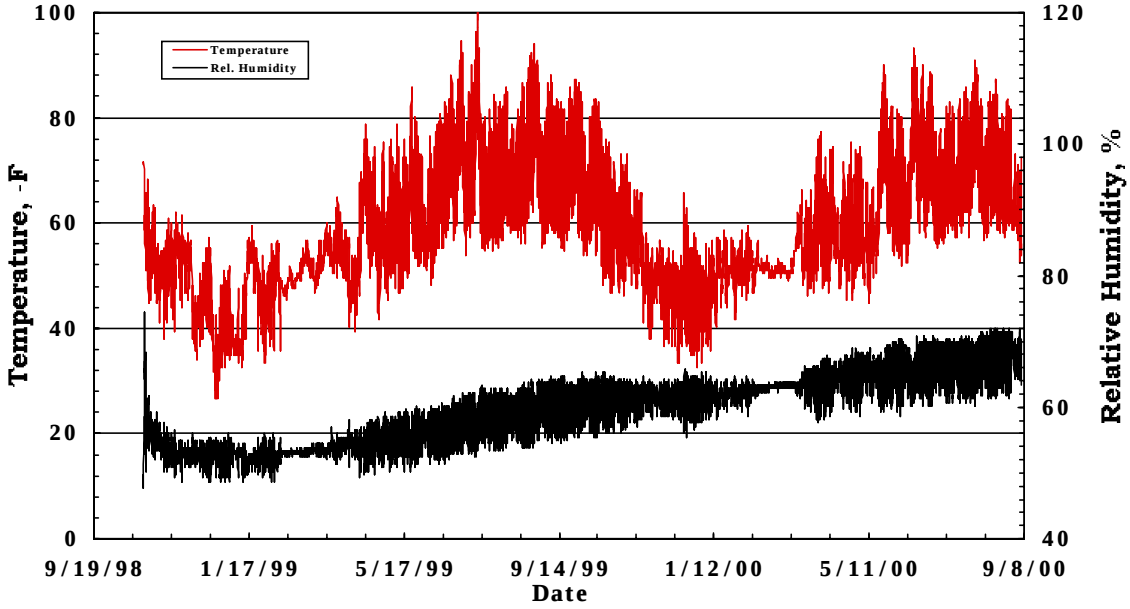

Figure 3.6. Temperature and relative humidity data taken once per hour on Column 8 of Bent 178. The sensors is located at the middle on the overwrap casing.

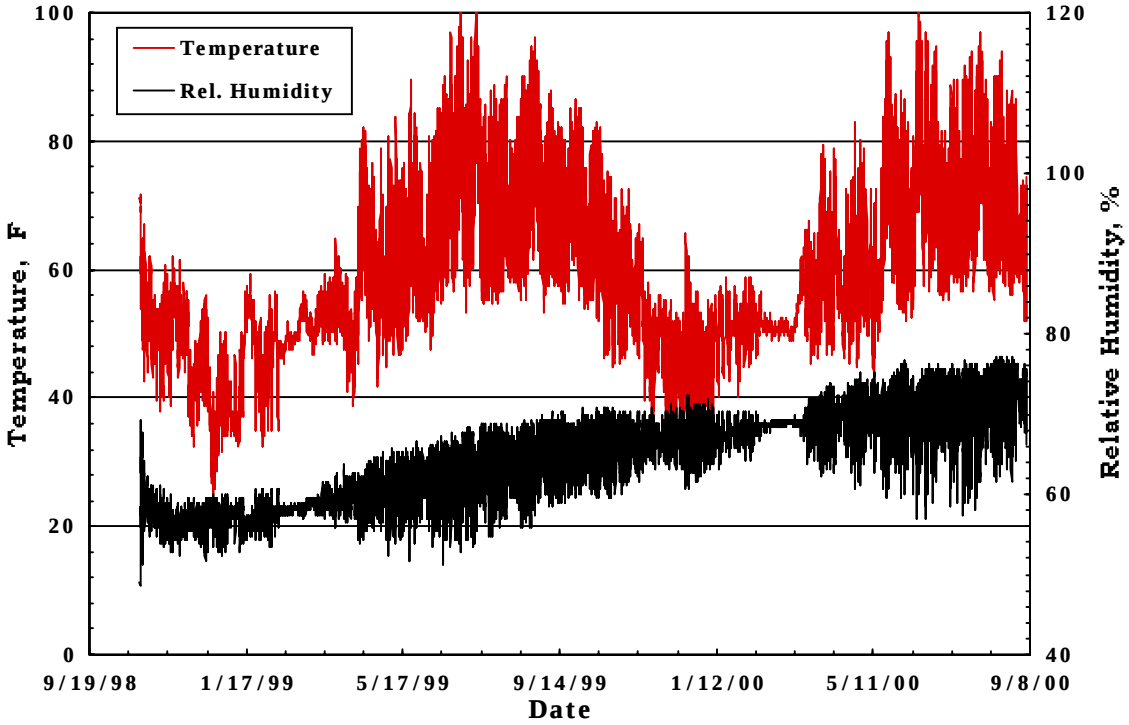

Figure 3.7. Temperature and relative humidity data taken once per hour on Column 12 of Bent 178. The sensors is located at the middle on the overwrap casing.

In general, all of the sensor data looks quite similar. The temperature data shows the daily night-to-day variation and is colder in the winter and warmer in the summer. In the late winter/early spring, the area is flooded, and the composite overwraps and the sensors are under water. This is evident in both the temperature and the humidity data because the day-to-night variation is much smaller during the period of flooding. The water stays a relatively constant 51°F, especially in February of 2000 when the water level was higher and stayed for a longer period than in 1999.

The temperature rising and falling on a daily basis is expected. What requires a further explanation is the concomitant rise and fall of the humidity measured by the sensors. As shown in Figure 3.1 the sensors are contained in a volume that is completely sealed, and (after an initial settling time) the only cause of humidity changes is from water vapor being absorbed or released by the concrete. It is not feasible that the amount of water contained in the concrete changes hourly, the apparent relative humidity changes must be due to another cause.

To answer this issue it is enlightening to look more closely at the humidity data. Figure 3.8 shows the portion of the temperature and humidity data taken over a five-day period in the summer of 1999.

It is apparent from the data that the temperature and the humidity data are out of phase with each other. The humidity data is falling when the temperature data is rising. To make sure this data is consistent, all of the sensors were studied at different time periods and they all showed the same effect. For example, the data in Figure 3.9 shows the same sensor in the winter of the same year when the temperature is much colder. The same effect is evident.

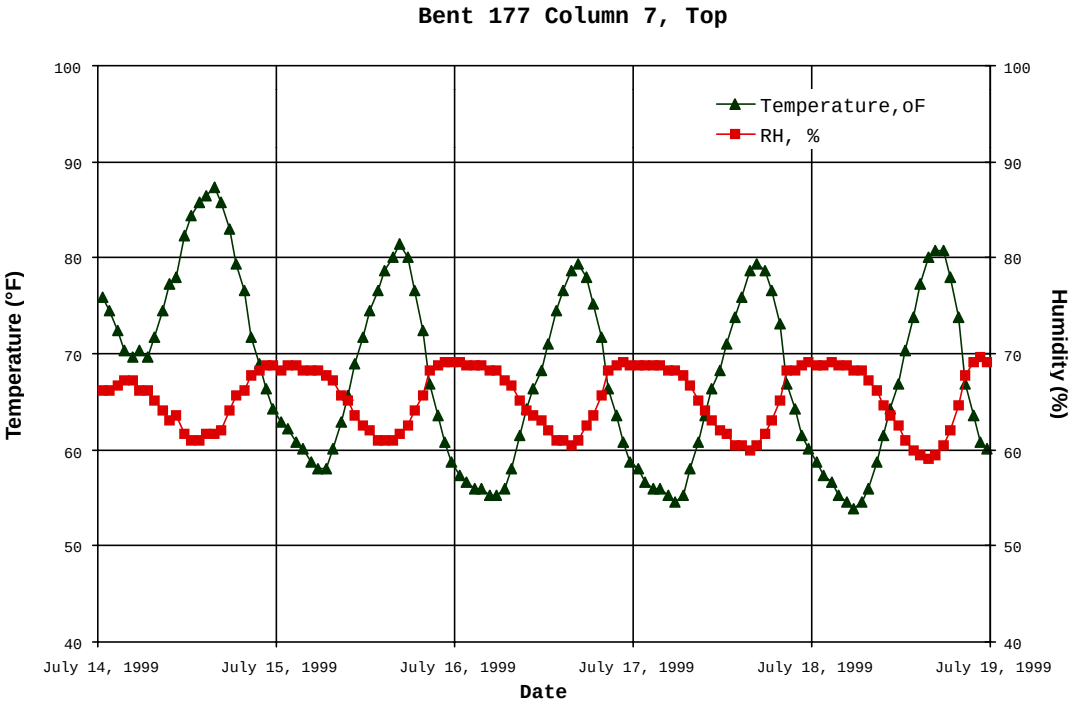

Figure 3.8. Typical temperature and relative humidity data taken during five days in the summer of 1999. The labeled dates indicate midnight at the beginning of that day.

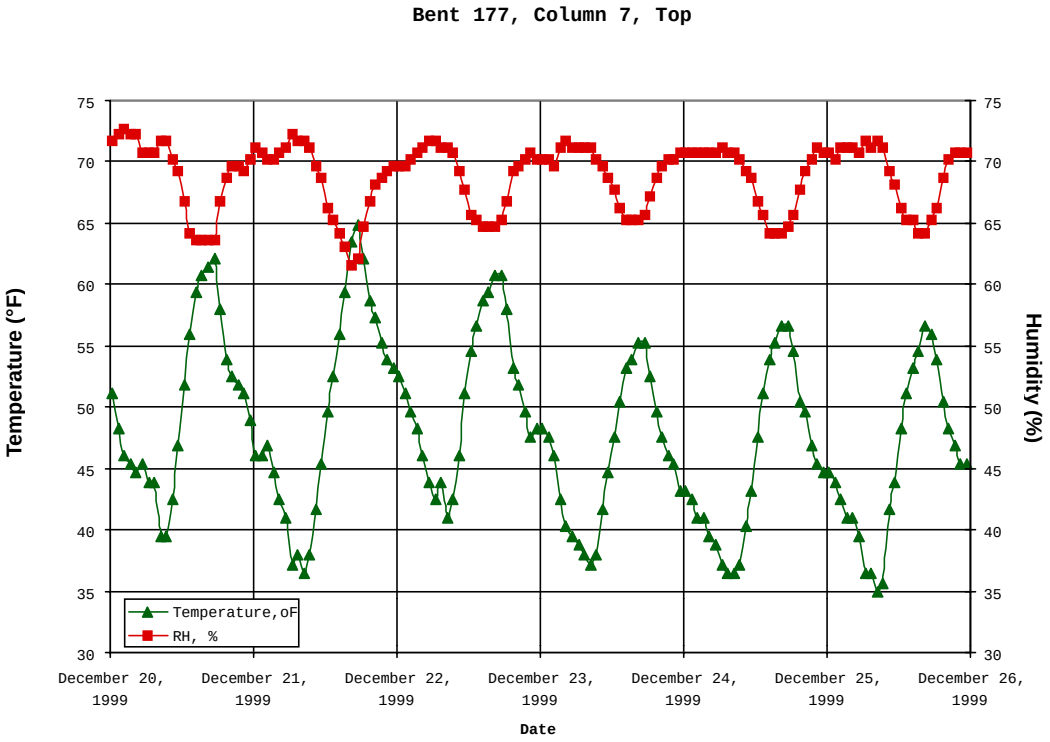

Figure 3.9. Typical temperature and relative humidity data taken during five days in the summer of 1999. The labeled dates indicate midnight at the beginning of that day.

These results can be understood by considering how the temperature affects the relative humidity in the gas in the sensor volume. If the volume were completely sealed and no moisture could come from the concrete, then the absolute humidity in the volume would be fixed, but the relative humidity would still change with temperature. Since warm air holds more moisture than cold air, when the amount of moisture is fixed, the relative humidity decreases as the temperature increases.

In other words, as the temperature rises, the air is able to hold more moisture. For the relative humidity to remain in equilibrium with the concrete, additional moisture needs to be added. The concrete cannot add the moisture quickly enough to keep the relative humidity in equilibrium; consequently, the relative humidity decreases. The opposite occurs when the temperature decreases causing the relative humidity to rise. In summary, the day-to-day variations stem from the concrete's inability to supply or extract moisture as quickly as the temperature changes.

To ascertain the concrete moisture level, we need to integrate the data over a specific time period to average out the daily variations. The integration period can be determined from the time constant of the sensor/concrete system. The required integration value turns out to be evident from inspecting the data. It can be seen by viewing the first few weeks of every dataset that the recorded humidity decreases for one to two months and then begins a continuous increase. This indicates that the sensor assembly required a month or two to come into equilibrium with the surroundings and begin measuring real values. Assuming this to be the case, a running average of a month of data was performed over the entire period. The results are shown in Figure 3.10.

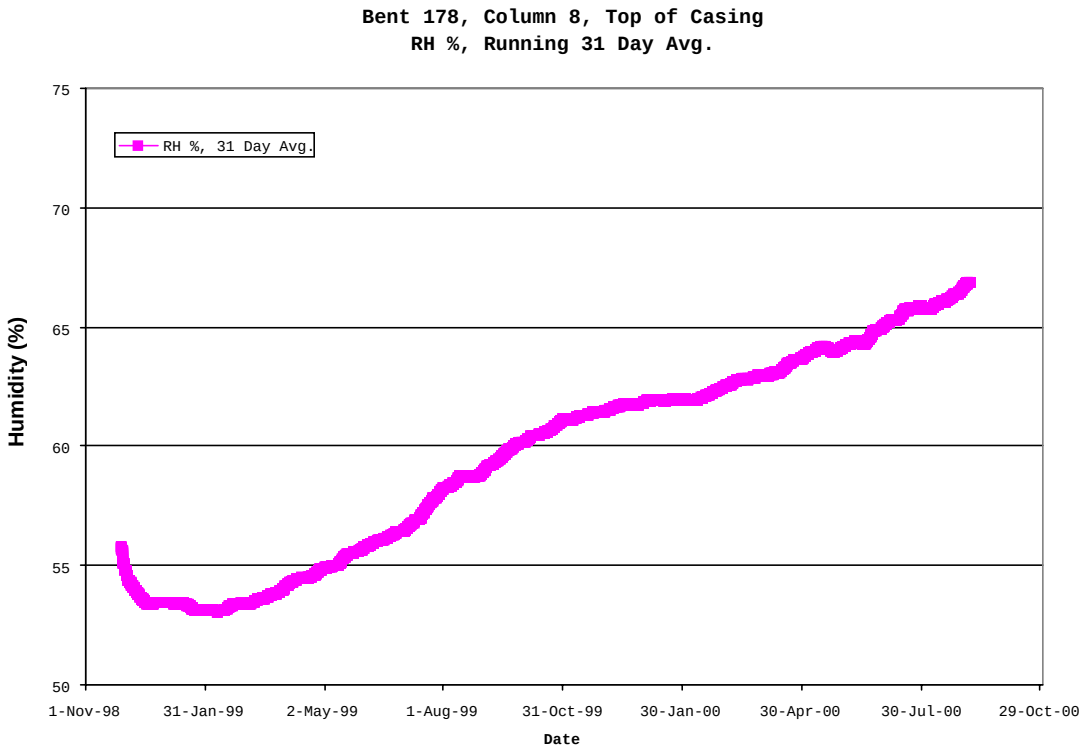

Figure 3.10. A 31-day running average of the relative humidity of column 8 in Bent 178.

The first thing that is evident from this data is that for the first six weeks, the sensor measures a decreasing humidity level. The humidity level reaches a minimum at the end of January when the area is flooded. After this initial dry-out period, the humidity monotonically increases for the remainder of the measurement period.

The initial dry-out period is due to the materials coming into equilibrium with each other. The sensor assembly, the composite material, and the adhesive used to bond the composite shells together had all been recently applied to the concrete. When compared to moisture uptake tests performed in the laboratory, it is not unusual to have a composite system require six weeks to come into equilibrium with its surroundings.

After the initial dry-out, the data in Figure 3.10 show how the humidity contained in the concrete increases with time over the remaining two-year period. The 31-day average seems to be the proper integration time because it did not smooth out all of the detail, yet it eliminated the day-to-day variations that confused the data interpretation.

The 31-day running average was calculated for all of the sensors, and the results are shown in Figure 3.11. As can be seen, the data from five of the sensors were essentially the same except for the data from the middle of column 3 on Bent 178. This particular sensor either is malfunctioning, or the seal may be violated, allowing an external source of moisture to affect the readings. Because the data are so different from the other five sensors, we will assume it is anomalous and not discuss it further.

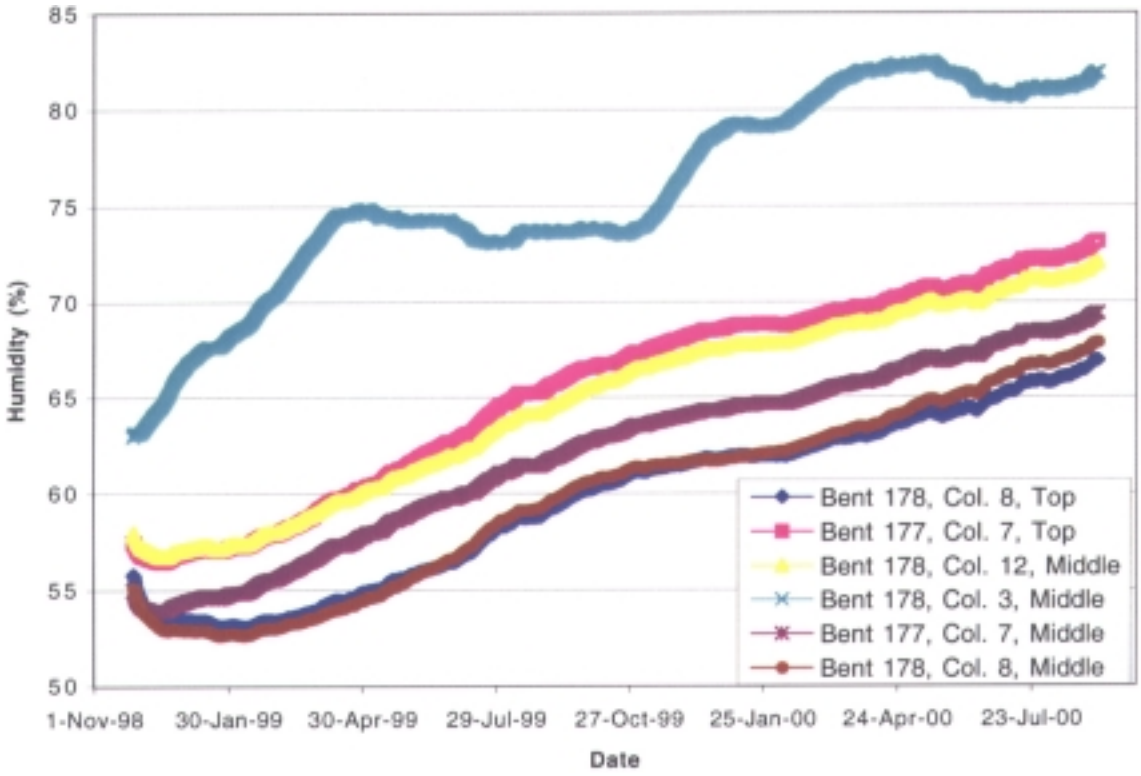

Figure 3.11. A 31-day running average of the relative humidity of all of the columns instrumented.

The water content of the columns increases throughout the first year with an indication of reaching a constant value in January of 2000. At that time, the area was flooded, and the water content increased again. This trend is uniform across the five different sensors and shows no sign of abating. We can only assume that the increase will continue until the columns are saturated with water.

3.5 Conclusions

This data has implications on the durability testing of composites for infrastructure applications. Adhesives need to perform for many years. Laboratories attempt to predict the useful lifetime of materials using accelerated methods to perform tests in a reasonable time. The accelerated test methods involve exposing the materials to high temperatures and humidity. Mechanical tests are performed on these samples, and the results are compared to control samples that have been kept in a benign environment. To extrapolate the test results and predict the material's lifetime, the conditions of the actual environment need to be determined. In addition, actual field condition monitoring determines whether the accelerated methodology is either benign or too severe.

This data shows that the current durability humidity tests are certainly not too severe. The composite material and the bondlines on the Yolo columns will soon be continuously saturated with water and are routinely being exposed to temperatures in excess of 100°F during the summer. The accelerated testing procedures will need to be reviewed in light of this data.

This page intentionally blank.

Section 4. Determining the Growth of Bondline Flaws

An important aspect of the fabrication process was the verification of the bond integrity within the composite sleeves. At the Yolo site, tap testing (i.e., sounding) of the composite sleeve was the standard inspection technique used by the contractor to monitor the composite integrity. Tap testing requires an inspector to strike the composite sleeve with a hammer while listening for changes in the pitch that might indicate voids.[1,2] Tap testing is a very fast and easy inspection that has been successfully applied to certain limited applications. However, as an inspection tool it suffers from several serious deficiencies that include, potential damage to the structure during testing, no ability to archive inspection data, low sensitivity to small or deep flaws, and dependence on the skill of the operator.

During this program, The Aerospace Corporation developed an Infrared (IR) Thermographic inspection technique that addresses the limitations of the tap test and other inspection methods currently in use for composite evaluation. By use of this technique, columns with debonded areas were identified in an initial survey conducted soon after the retrofitting was completed. The debond dimensions were noted, and the same columns were tested yearly for two years. This section describes the thermographic technique as applied to columns and the results of the multiple thermographic tests.

4.1 Infrared Thermography

Infrared (IR) Thermographic inspection techniques utilize localized changes in the thermal characteristics of a structure to indicate the presence of subsurface defects. This type of inspection technique has several important advantages over other standard nondestructive evaluation (NDE) techniques such as tap testing (sounding), ultrasonics, and radiography. These advantages include fast data acquisition and evaluation, simple inspection procedures, and excellent sensitivity to voids and delaminations in composite structures. Thermography has become a standard tool within the aerospace industry for detecting delaminations and debonds within thin composite structures. The application of thermography to infrastructure applications required the technique be extended to the inspection of much thicker composites located in hostile field conditions.

4.2 Background of Thermographic Inspections

A typical thermographic inspection is initiated by creating a temperature gradient through the structure by either heating or cooling the target surface. The surface of the structure is then monitored for spatial temperature variations as it returns to thermal equilibrium. These spatial variations can be an indication of internal flaws such as unbonds and delaminations that tend to increase the thermal impedance of the structure. The enhanced thermal impedance due to a defect can result in localized surface temperature differentials ranging from less then 0.5°C to more then 3°C, depending on the flaw depth and the thermal characteristics of the structure. A schematic representation of a thermographic inspection is illustrated in Figure 4.1.

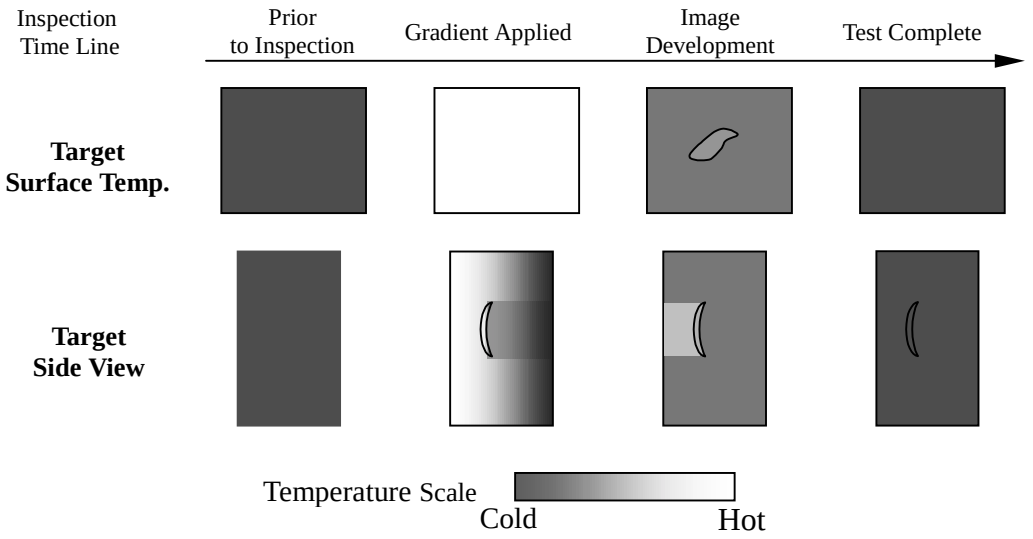

Figure 4.1. Schematic representation of a typical IR inspection of a structure containing an internal void.

4.3 Infrared Imaging Cameras

The two critical components of a thermographic inspection system are the IR camera and heat source. There are several commercially available IR cameras that have both the temperature and spatial resolution required to detect the small temperature changes indicative of a subsurface flaw. The primary IR camera used for the inspections of the Yolo causeway columns was a Radiance 1 manufactured by Amber Inc. The Radiance 1 utilizes a 256 x 256 indium antimonide (InSb) array with an onboard Sterling-cycle cooler. Sensitive to wavelengths between 3 and 5 μm, this unit has a documented thermal resolution of 25 mK. Initial evaluation work done both in the Aerospace NDE Laboratory and at the CalTrans demonstration site under the I-10 freeway in Los Angeles showed the performance characteristics of the camera exceeded the requirements for inspecting the columns under the Yolo causeway.

One of the drawbacks to using the Amber imager is its expense. The unit sells for ~$75K when applicable lenses are added to the cost. Some preliminary experiments were performed at the Yolo causeway to evaluate the capabilities of less expensive cameras to perform the inspections. A FLIR 570 camera manufactured by Agema, which sells for less then half the cost of the Radiance 1, was used for comparison purposes. The FLIR 570 is battery operated and utilizes a 320 x 240 pixel uncooled micro-bolometer detector operating over a spectral range of 7–13 μm. In addition to the lower cost, the FLIR camera has a faster startup time (~20 s). This compares to a startup time of ~15 min for the Radiance 1. The temperature resolution of the FLIR camera is ~0.1°C, which is significantly lower then the Amber unit. The effect of the lower resolution can be seen in Figure 4.2 where the same indication is imaged with both the FLIR 570 and the Amber Radiance 1. The indication is visible in both images, but the boundary is less defined in the FLIR image than the Amber image. Note that the FLIR is radiometrically calibrated such that actual surface temperatures can be recorded, provided the emmitance of the target is known. The Radiance 1 does not have this capability. The

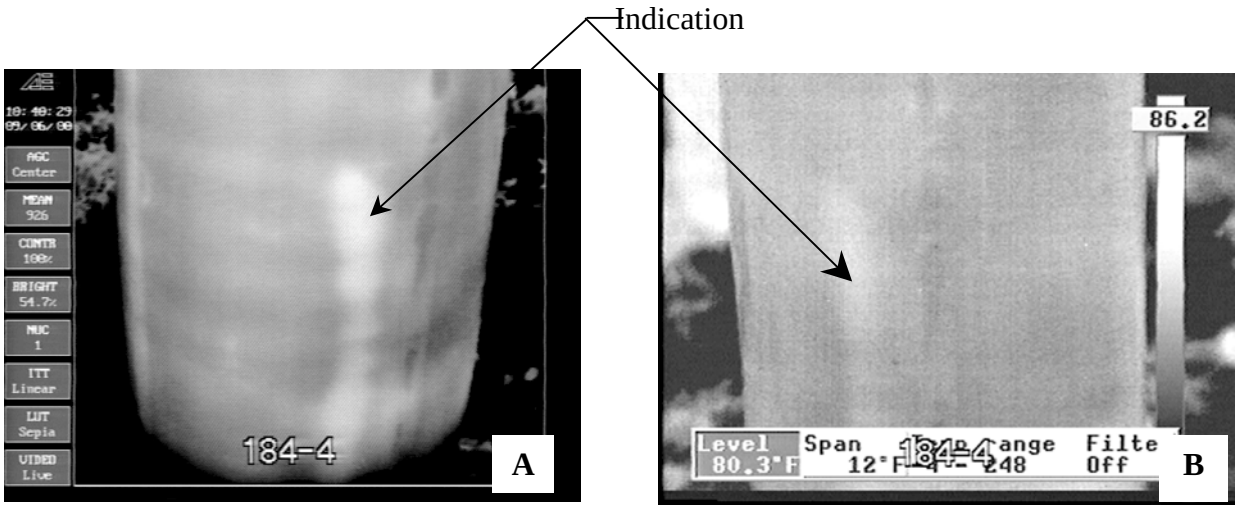

Figure 4.2 Comparison of images of the same indication from (a) Amber Radiance 1 camera and (b) the FLIR 570 Camera.

preliminary results suggest that the lower cost camera could perform the Yolo inspection satisfactorily. Additional work would be required to ensure comparable sensitivity to a wide range of defect sizes and depths.

4.4 Thermal Loading

The second element of a successful IR inspection procedure is the uniform heating of the target surface. This minimizes inspection uncertainties due to thermal variations in the initial loading of the target specimen. Common methods for heating the target surface include heat lamps, heated water, solar energy, and flash lamps. The selection of a particular heating technique depends on the both the thermal

properties of the structure and the inspection requirements (defect sizing and depth resolution).[3] For retrofit applications on concrete substrates, radiant heating provided the best combination of convenience, cost, and expandability. Low-power (<500 W) quartz halogen bulbs are the basic heating element for retrofit inspection systems. These bulbs have an active length of ~3 in., are readily available and inexpensive, and the total output power can be sized for a specific application. In 1999, a dedicated heat source was designed to meet the requirements of the Yolo causeway. Shown in Figure 4.3, the heater can use up to 12 300-W lamps to generate a consistent thermal gradient across the composite sleeve with a single pass of the heater.

A small drive motor is included in this design to aid in the uniform deposition of the thermal energy. The drive speed could be adjusted during the initial set-up to provide adequate lamp dwell times during the column heating.

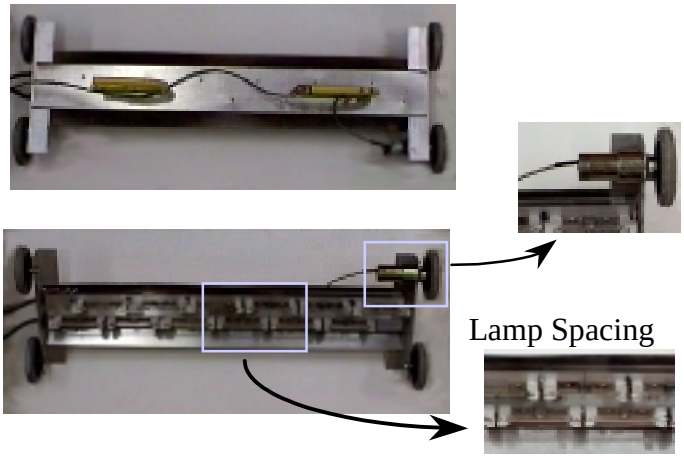

Figure 4.3. Heater designed for use with the columns in the Yolo causeway.

4.5 Experimental Procedure

4.5.1 Column Identification

The experimental procedure for the inspection of the columns evolved over the course of the three-year investigation. This was an expected part of the development program, incorporating lessons learned from each trip to the Yolo causeway. However, as a result of these changes, it can be difficult to make direct comparisons between the data collected from year to year. Where applicable, changes in the inspection procedure will be noted in the data along with the reason for the change.

The large number of columns that were wrapped (>3000) and the limited time available to complete the task necessitated a sampling approach to the testing. Twenty-eight columns were randomly selected for inspection during the initial experimental evaluation. The locations of the individual columns are identified by bent and column numbers. The bent number identifies a unique row of 12 reinforced columns supporting the freeway. The reinforced columns were numbered from 1 to 12, starting from the southern edge of the causeway. The numbering scheme is illustrated in Figure 4.4.

The columns to be inspected were selected from a variety of locations both along the causeway and within a particular column bent.

In the subsequent inspections, emphasis was placed on the re-inspection of columns that had significant indications. A few additional columns were examined to evaluate inspection timing issues. A tabulation of the columns inspected and the occurrence of indications larger then 20 cm^2 (~3 in^2) is provided in Table 4.1. Indications as small as 10cm^2 were detected but were not recorded as part of this investigation.

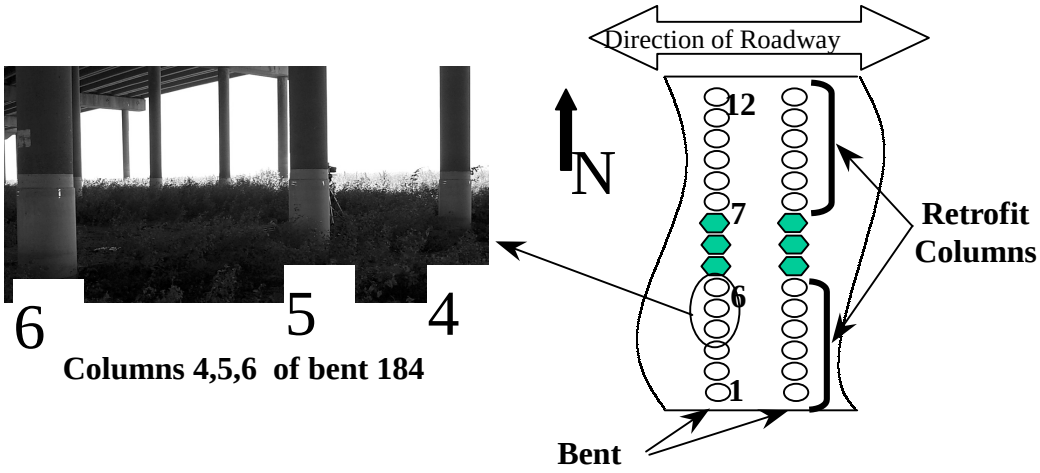

Figure 4.4. Identification of specific columns during the inspection process by bent and column number

Table 4.1. Columns Inspected Over the Course of the Evaluation Program

Yolo Causeway Columns Inspected				
Location		Year		
Bent	Column	1998	1999	2000
59	2			
67	7	(I)		(I)
70	10			
107	3			
107	4			
107	5			
107	9			
107	10		(I)	(I)
133	4			
133	5	(I)		(I)
133	6	(I)		(I)
133	7			
170	9			
170	10	(I)		(I)
182	3			
184	4	(I)	(I)	(I)
184	5	(I)	(I)	(I)

Location		Year		
Bent	Column	1998	1999	2000
184	6	(I)	(I)	(I)
190	12			
196	7			
196	8			
196	9			
207	6			
262	2			
262	3			
262	5			
264	3			
211	8			
273	5			
273	6			
280	3			
284	3			
284	4			

(I) Indications (< 20 cm^2), ( ) inspected

Yolo Causeway Columns Inspected

In addition to identifying a specific column, it was also necessary to record the directional orientation of each image to ensure the comparison of similar views on subsequent inspections. For the initial 1998 inspections, the orientation was recorded in a written log of the inspection as well as onto the image in the Hi-8 video recorder using the manufactures captioning tool. This recording process proved to be cumbersome at best and prone to errors. In the subsequent inspections, only the bent and column number were digitally stored on the inspection image. Tape markers applied to the face of the column provided orientation within the image. These markers were clearly visible during the inspection process, as illustrated by the East Face of column 5 bent 184 shown in Figure 4.5.

4.6 Inspection Coverage

Prior to inspection, the IR camera was mounted to a tripod along with a Sony Hi-8 video recorder. The Hi-8 has S-video recording resolution in a small, low-power camcorder unit. For typical inspections, the tripod was positioned ~4 ft from the column. This offset provided appropriate coverage of the column when using the standard 28-mm lens with the Radiance 1 camera. The column identification (bent, column) was entered into the caption tool of the camcorder, and the orientation markers applied to the column. The thermal gradient was applied to the structure, and the camcorder recorded the IR image generated by the IR camera. An image of the inspection system is shown in Figure 4.6.

Typical test times from heating to final image evaluation were ~3 min. During the image development, the IR camera was moved into different positions around the column to get 100% coverage of the composite sleeves. Moving the camera during the image development saved significant inspection time, but at a cost of depth information for the indications. The camcorder images were used to evaluate the column and provide an archive of the image data. Figure 4.7 is an example of a typical image acquired from the Hi-8 camcorder.

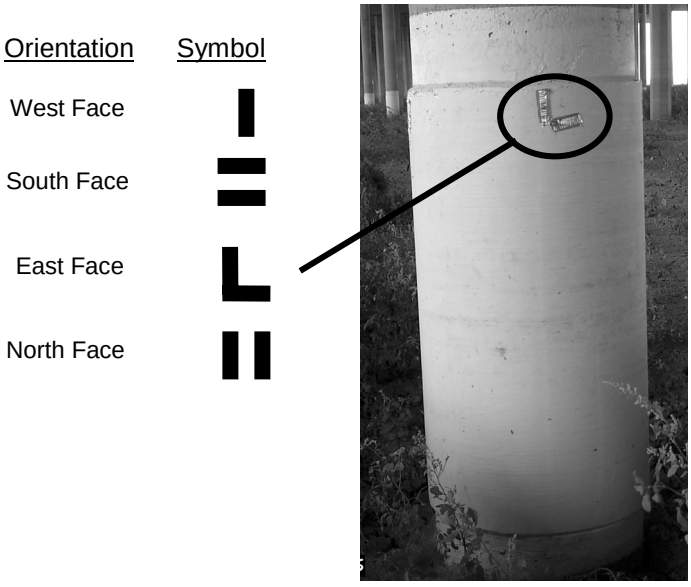

Figure 4.5. Orientation marker for IR images of the reinforced columns. The markers were readily visible in the initial frames of the inspection aiding in the comparison of subsequent inspection images.

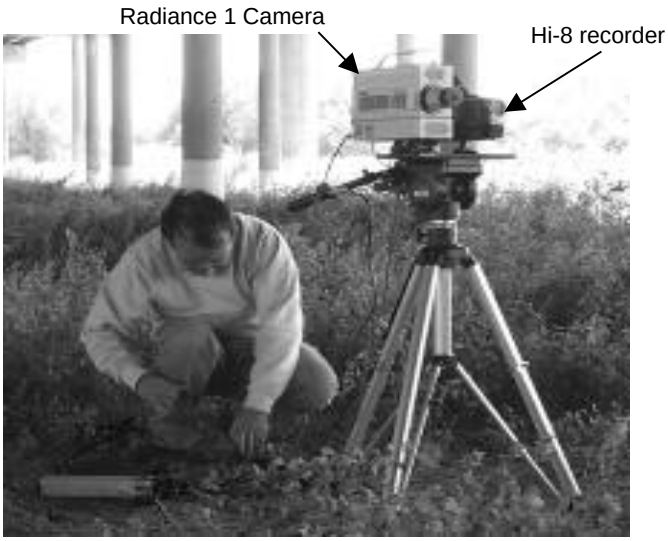

Figure 4.6. Imaging system comprised of both the Radience 1 IR imager and the Hi-8 video recorder.

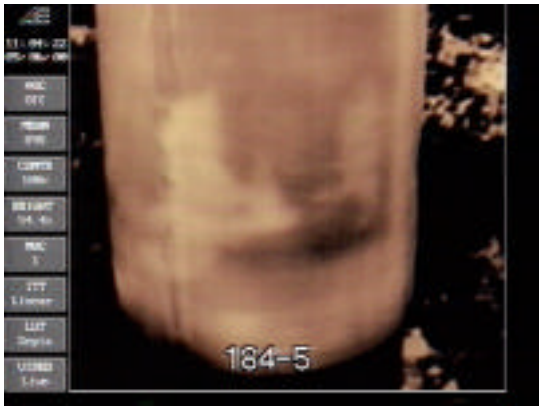

Figure 4.7. Typical IR image of a reinforced column. Note the caption with bent and column number. The information on the left hand side of the image is related to different camera parameters.

While the actual test duration was relatively short, the necessity of packing the equipment and moving it to the different bents increased the per column testing to ~30 min per column. In 1999, testing was performed that showed that column inspection times could be maintained at 2 min per column along a single bent, where the equipment shuffling could be held to a minimum.

4.7 Column testing

The composite casings were constructed using prefabricated epoxy/vinylester resin E-glass shells. A total of four casings, each ~0.1 in. thick and 2.5 ft long were layered on to the column. Each shell

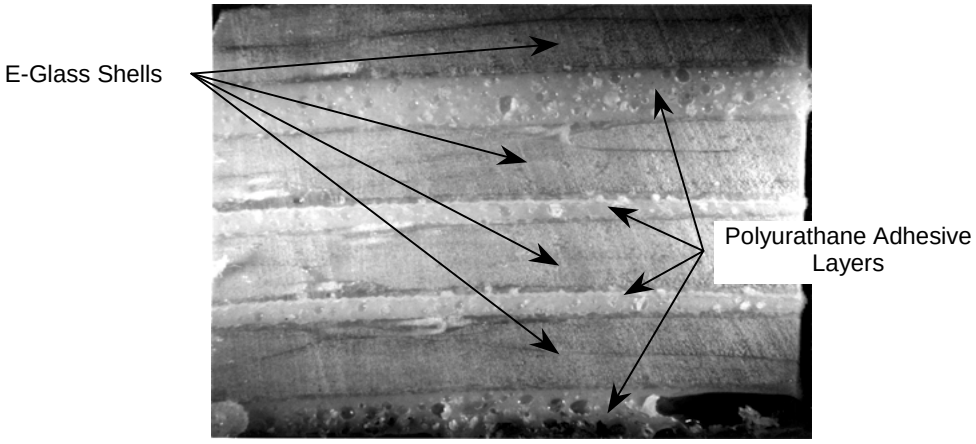

Figure 4.8. Cross-section of E-glass/epoxy sleeves bonded into a complete assembly.

was bonded to the underlying casing with a polyurathane adhesive for a total casing thickness of ranging from 0.5 to 0.75 in. A cross-sectional image of the complete composite casing is shown in Figure 4.8.

The completed assembly was then put under compression using a sequence of metal bands. After ambient temperature curing of the adhesive, each casing assembly was inspected for voids by a CA State inspector using the sounding technique. Voids located during the initial inspection were repaired using a "drill and fill" procedure whereby fill and vent holes are drilled into the suspect area, and adhesive is injected into the void. Both the banding and the column repair are shown in Figure 4.9.

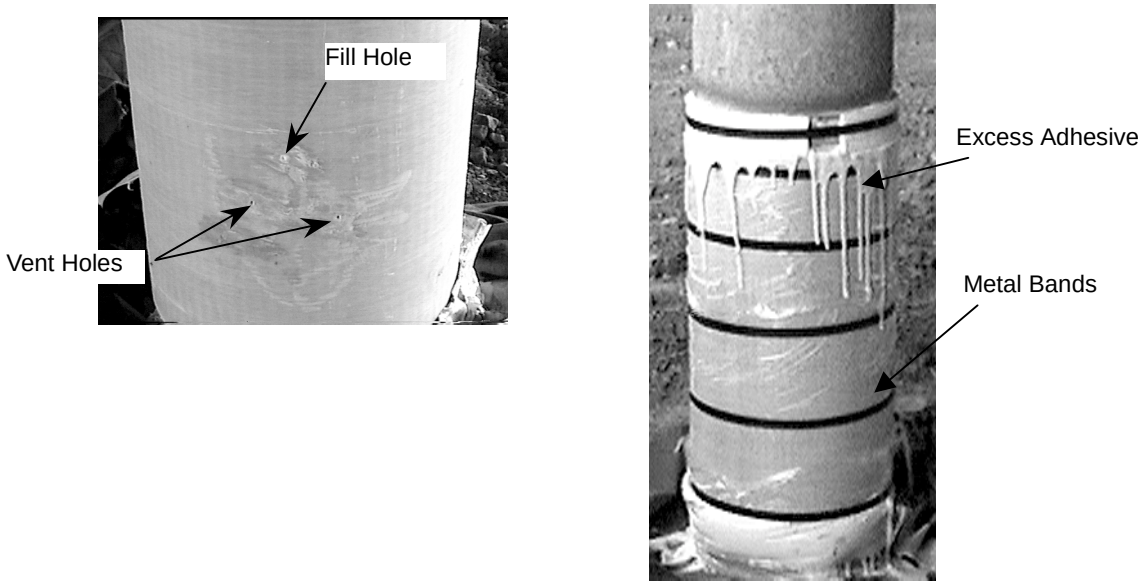

Figure 4.9. Aspects of the retrofit case assembly and repair.

4.8 Results

4.8.1 Background

An initial inspection of the selected reinforced columns was completed in October of 1998. A second inspection was completed in September of 1999, and the third and final inspection was completed in September of 2000. All of the inspections were recorded on videotape for archiving and future review. The images of indications from each column were digitized, and the surface area of the indication measured using the National Institutes of Health (NIH) public domain software Image 1.62. In the population of 30 columns inspected there were 8 columns with voids that measured larger then 20 cm^2. It is important to note that that these were indications that were not repaired during the tap testing. It is not clear whether the indications were missed or simply determined to be minor. In fact, this uncertainty highlights one of the significant drawbacks of sounding inspections: there is no provision for future review of the data. An example of a particular indication imaged over the course of this investigation is provided in Figure 4.10. Additional images are provided in Appendix II.

In order to determine whether a specific indication had changed over time, two inspection criteria had to be met: (1) confidence that the same indication was being compared year to year, and (2) any apparent change in the indication was larger then the inherent uncertainty in the measurement.

The first criteria was met in two ways: direct comparision between views as recorded on the inspection tapes, and noting distinctive characteristics of the indication. As mentioned previously, changes were made in the data recording to help ensure that the comparisions were made between the same columns and camera orientations.

Variations in the measured indication areas can be related to a number of factors, including year-to-year changes in the inspection procedure, and uncertainty in the image intensity can have some impact on the boundries of the indications. Based on the experience gathered from these inspections,

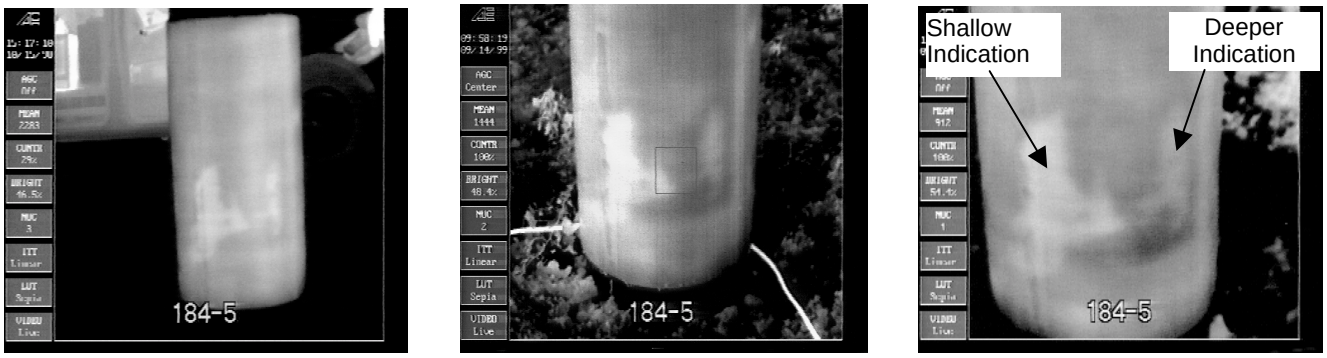

Inspection Date 1998
Area of Indication 225 cm^2

Inspection Date 1999
Area of Indication 215 cm^2

Inspection Date 2000
Area of Indication 223 cm^2

Figure 4.10. IR images of a specific indication acquired over a period of 3 years. The areas of interest appear as light regions on the composite sleeve..

an increase in the area of more then 25% in the measured area would be required to demonstrate growth in a particular indication. Figure 4.11 is a representation of the measured areas of the unbond indications. None of the eight columns showed a significant increase in the indication area. This suggests that the time scale required for environmental water to infiltrate the columns and increase the unbonded area is longer than 3 years.

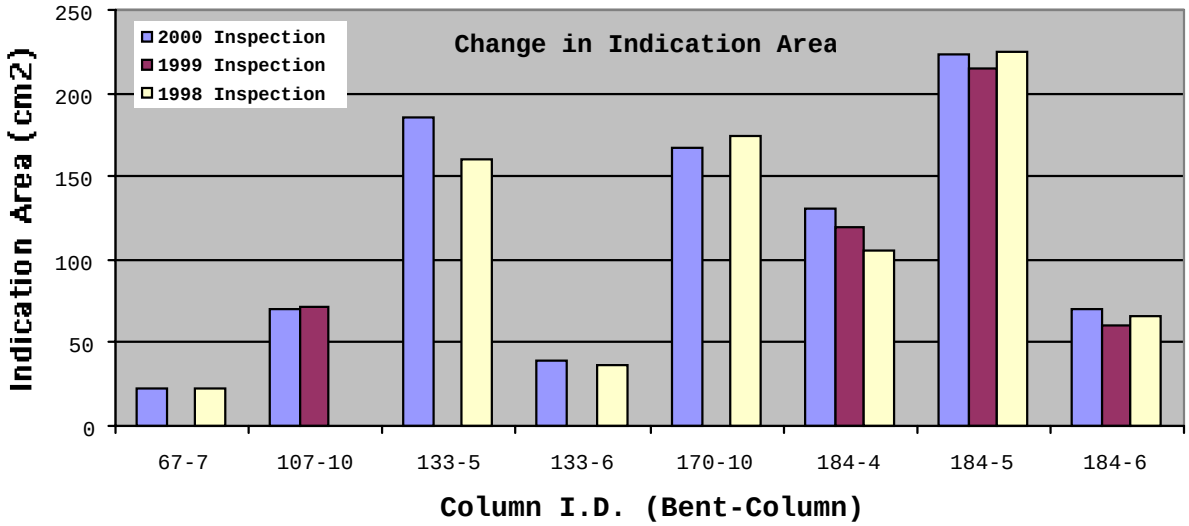

Figure 4.11. Comparison of measured indication areas over the course of the 3-year investigation.

4.9 Conclusions

The Nondestructive Evaluation (NDE) Section of The Aerospace Corporation evaluated a random sampling of 30 reinforced columns, looking for internal unbonds related to the construction process. The initial inspection of the columns was done in October of 1998. The columns were inspected using an Infrared (IR) thermography technique developed at The Aerospace Corporation. The result of these inspections confirmed that thermography is a sensitive method for detecting unbonds larger then 20 cm^2 in the composite casing. Additional work could be carried out to improve different aspects of the inspection procedure. This work might include developing the capability to easily find the depth of the indication as well as increasing the inspection rate. However, as currently implemented, thermography has significant advantages over the sounding technique. Specifically, it has the ability to archive the inspection results and generate accurate maps of the indications. The principle drawback to thermography is its relatively high initial equipment cost.

From the random sampling of 30 columns, ~25% were found to have indications larger then the threshold value of 20 cm^2. Over the complete Yolo span, this implies that over 700 columns might have been accepted with reportable indications. The indications were monitored for changes in area over the three-year study. None of the identified flaw areas increased over this time frame. A valuable follow on program would include the inspection of these columns on some longer-term schedule, possibly as often as every three years.

4.10 References for Section 4

1. P. Cawley and R. D. Adams, “Sensitivity of the Coin-Tap Method of Nondestructive Testing,” Materials Evaluation 47, May 1989, pp 558-563.

2. D. Hagemaier and R. Fassbender, “Nondestructive Testing of Adhesively Bonded Structures,” SAMPE Quarterly, Vol. 9, July 1978, pp 36-58.

3. V. P. Vavilov and X. Maldague. “Optimization of Heating Protocol in Thermal NDT, Short and Long Heating Pulses: A Discussion,” Res Nondestr Eval **6**: 1-17 (1994)

This page intentionally blank.

Appendix I—Determining Whether Fourier-Transform Infrared Spectroscopy Can Be Used to Monitor Yolo Bondline Degradation

Background

Samples of composite material used for the retrofit program were provided to The Aerospace Corporation for evaluation under a variety of long-term exposure conditions consistent with the Yolo Causeway environment. Among these conditions were ambient immersion in alkali, elevated-temperature exposure, and elevated-temperature exposure with humidity. An additional exposure of 20 freeze/thaw cycles was also used. Samples were exposed to these conditions for a maximum of 10,000 h. The focus of this task was to use fiber-optic sensors to monitor changes in bondline performance using Fourier-transform infrared spectroscopy (FTIR).

Results

Polyurethane adhesive MOR-AD 695-28 was the adhesive used for the composite retrofit. Composite samples were subjected to a number of exposure conditions, as described in Table I. These conditions were selected based on conditions that would normally be expected at the Yolo Causeway site. The conditions selected were alkali exposure, resulting from concrete used in construction, elevated temperature and humidity conditions from prevailing weather, and a freeze/thaw cycle. These conditions were used to evaluate the effects of environmental exposure on the mechanical properties of the composites. As a follow-up to this evaluation, samples of adhesive from each composite exposed to the conditions defined in Table I were also analyzed by FTIR.

The results for Group I samples exposed to an alkaline environment of approximately pH 9.5 are shown in Figure I-1. In general, the spectra for samples exposed for up to 10,000 h are little changed from that of the control sample. Minor changes observed in the fingerprint region of the spectra (below 1000 wavenumbers) are deemed insignificant and confirm the consistency of the mechanical property test results observed for these samples.

The results for the Group II samples exposed to elevated temperature are shown in Figure I-2. Again, except for minor differences in the fingerprint region below 1000 wavenumbers, the FTIR spectra of the adhesives exposed for up to 3000 h at 140°F are essentially unchanged from that of the control.

Similarly, for Group III samples exposed to both elevated temperature and humidity, the FTIR spectra of the adhesives exposed for up to a 3000 h are essentially unchanged from that of the control. Even after the 10,000-h exposure, the specrum of the sample is relatively unchanged in the region above 1200 wavenumbers. Differences in the fingerprint region below 1200 wavenumbers are the most pronounced of all the exposure conditions under which the adhesive was subjected. Although this result has not been significant enough to impact the mechanical property results through this time period, it may be an initial indication of degradation that might occur over a much longer exposure period. The results are seen in Figure I-3.

Table I. Polyurethane Adhesive Environmental Exposure Conditions

Group I

FP 29 B3	Control		
FP 29 B1	ambient	alkali	1000 h
FP 29 B2	ambient	alkali	3000 h
FP 42 B4	ambient	alkali	10000 h

Group II

FP 34 A4	Control		
FP 34 A2	140°F		1000 h
FP 34 A1	140°F		3000 h

Group III

FP 17 A1	Control		
FP 17 A2	100°F	100% RH	1000 h
FP 17 A3	100°F	100% RH	3000 h
FP 17 A4	100°F	100% RH	10000 h

Group IV*

FP 34 A3	Freeze	0°F	8 h
	Thaw	100°F/100% RH	16 h

*Sample equilibrated for 3 weeks at 100°F and 100% RH followed by 20 freeze/thaw cycles

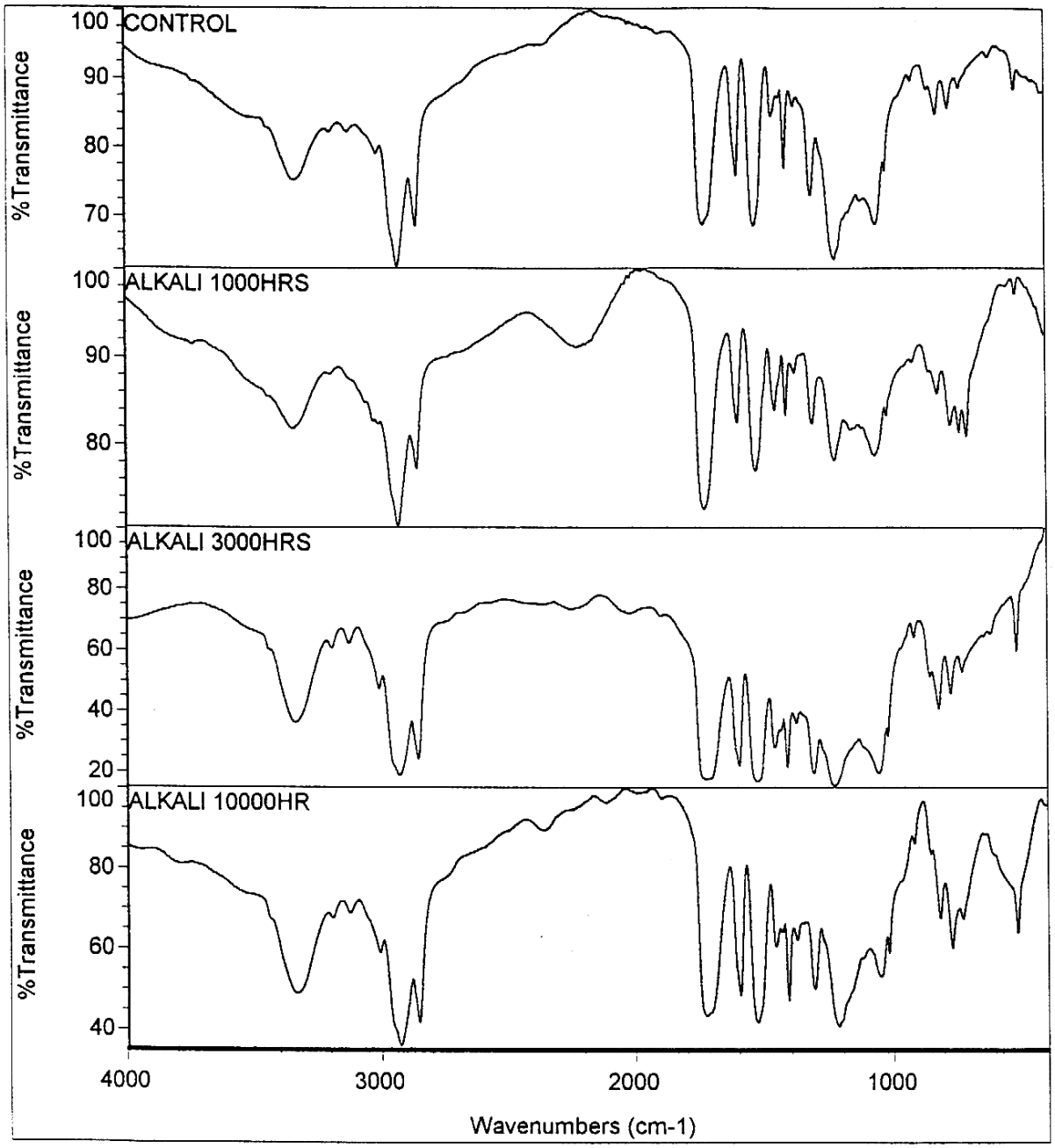

Figure I-1. FTIR transmission spectra for adhesives from composite samples exposed to alkaline conditions.

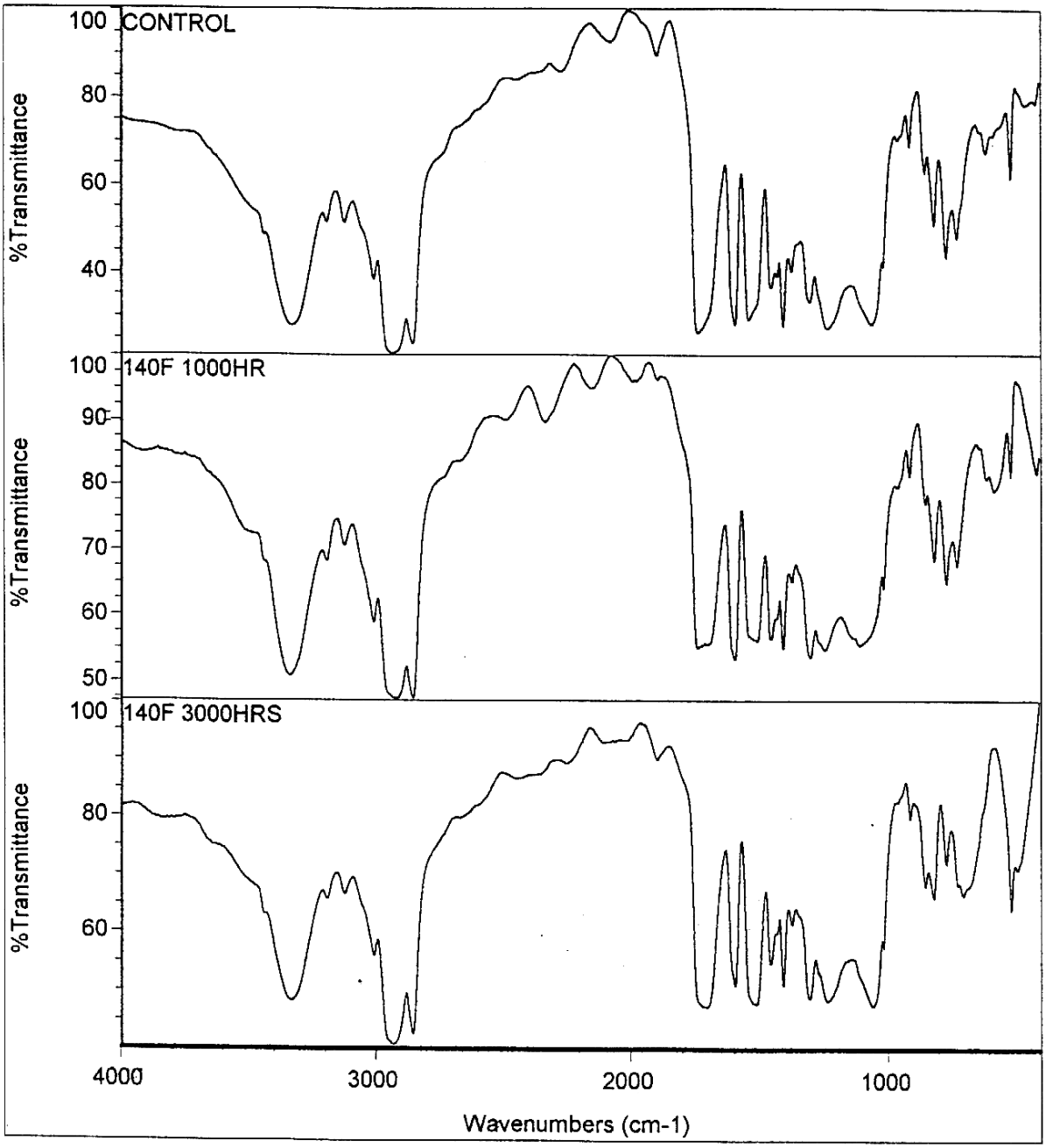

Figure I-2. FTIR transmission spectra for adhesives from composite samples exposed to conditions of 140°F and ambient humidity.

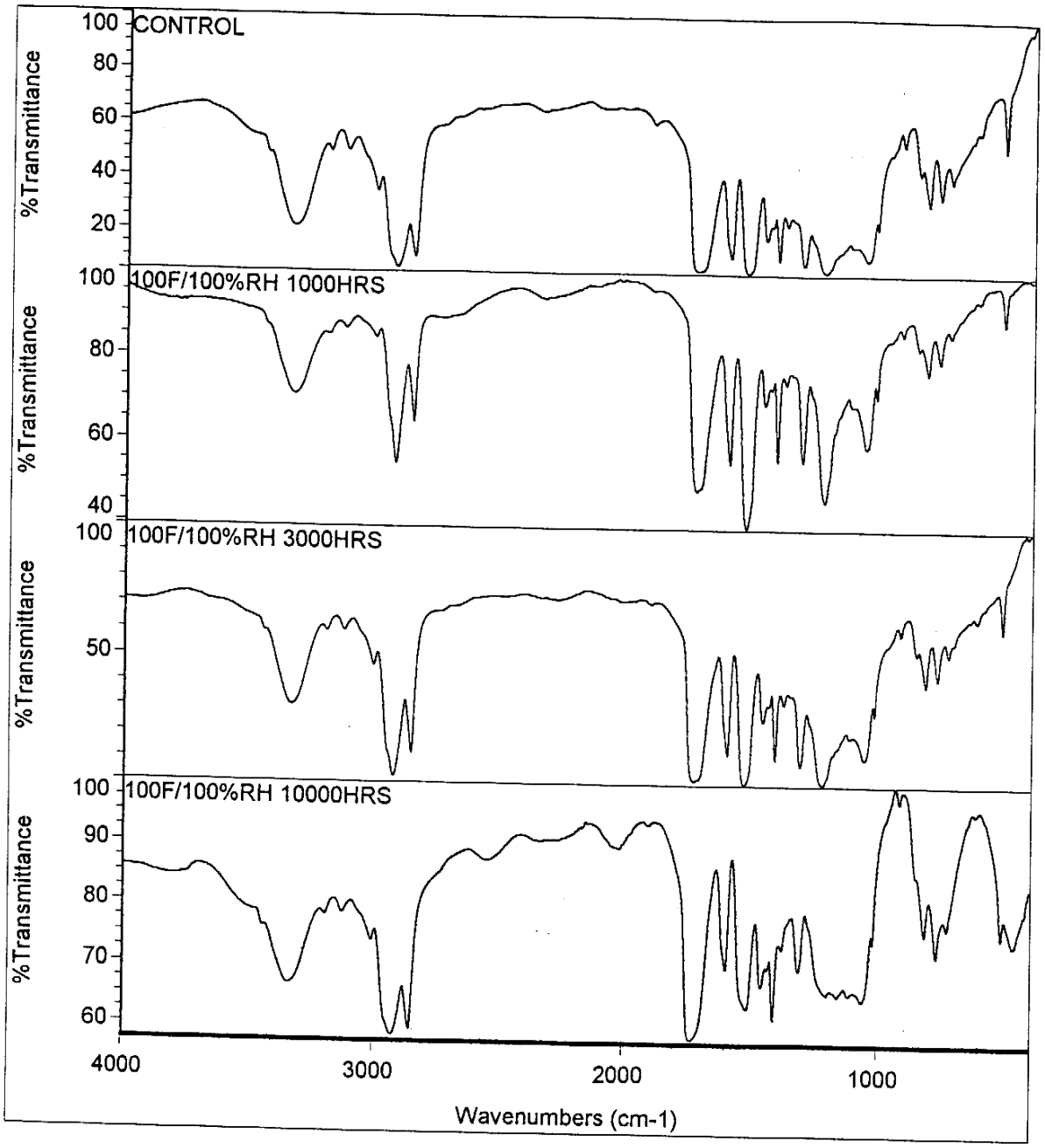

Figure I-3. FTIR transmission spectra for adhesives from composite samples exposed to conditions of 100°F and 100% RH.

A single sample of adhesive was also subjected to a freeze/thaw cycle that would be common during a 24-h winter period. Again, no major change in the FTIR spectrum was observed when compared to that of a control. The spectrum is shown in Figure I-4.

Similar to the results observed for the long-term exposure conditions described for Groups I, II, and III, the sample in Group IV was also little changed following the prolonged thermal cycling conditions expected to prevail during seasonal extremes. The only distinct similarity with the other Groups was that the fingerprint region below 1200 wavenumbers in Figure I-4 was consistent with that of the Group III exposure of 10,000 h in Figure I-3. This may be the earliest indication that changes in the FTIR spectra are the result of an aging process that contributes to long-term degradation of the adhesive material. Because of the small changes observed during the time period studied, these results precluded the use of FTIR fiber-optic sensing for the Yolo Causeway project.

Conclusion

Aging processes of the kind to be experienced by the composite retrofit materials are expected to be slow, but cumulative changes over time should easily be observed by standard FTIR techniques. However, in-field monitoring by fiber optics using state-of-the-art remote sensing equipment suffers a greater than 70% loss in sensitivity from that analyzed directly. It was concluded that long-term aging of adhesives within these composites would exhibit changes too small to be detected by remote sensing using the FTIR technique.

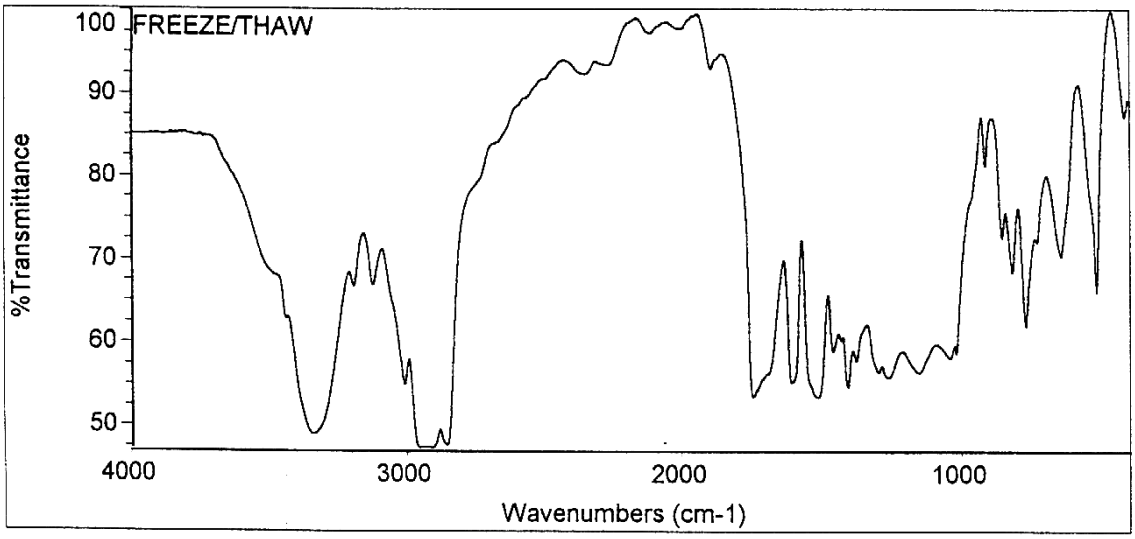

Figure I-4. FTIR transmission spectrum for adhesive from composite sample exposed to a freeze/thaw condition.

Appendix II—IR Images of Selected Columns

Column 7 Bend 67

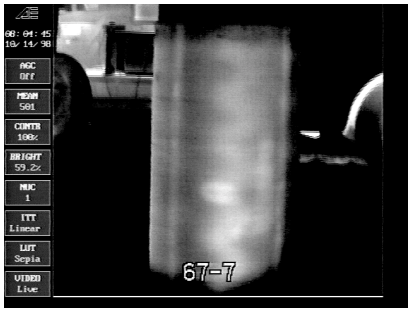

Inspection Date 1998
Total Area of Indication 192 cm^2

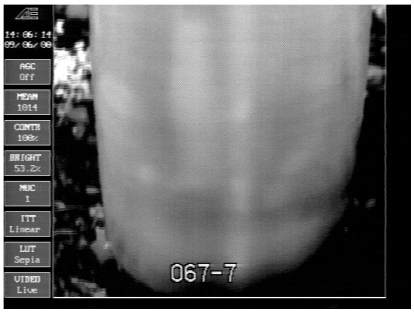

Inspection Date 2000
Total Area of Indication 193 cm^2

Column 10 Bent 107

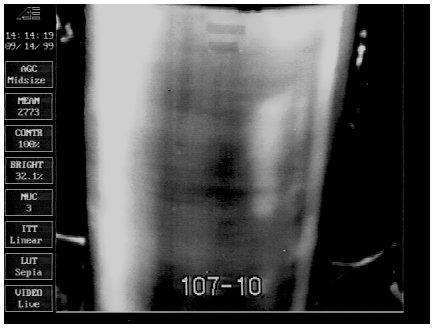

Inspection Date 1999
Area of Indication 73 cm^2

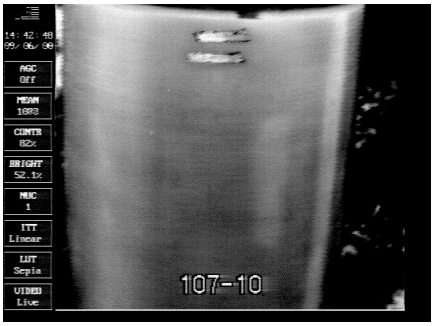

Inspection Date 2000
Area of Indication 73 cm^2

Column 5 Bent 133

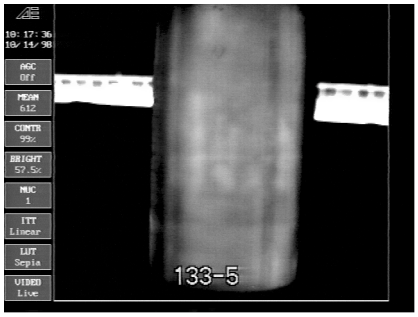

Inspection Data 1998
Area of Indications 185 cm^2

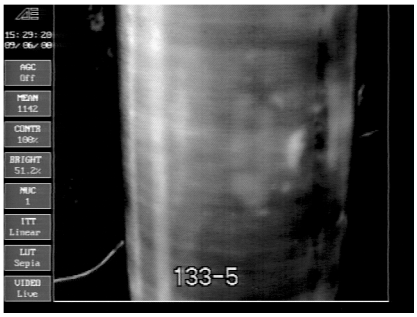

Inspection Data 2000
Area of Indications 160 cm^2

Column 6 Bent 133

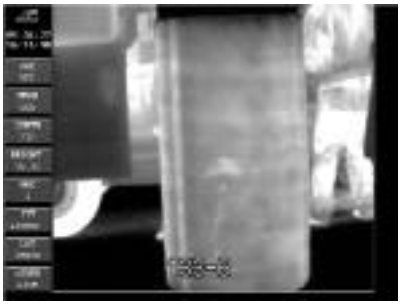

Inspection Data 1998
Area of Indications 40 cm^2

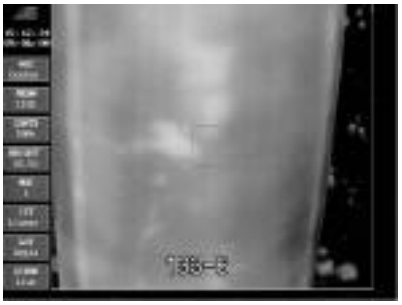

Inspection Data 2000
Area of Indications 36 cm^2

Column 10 Bent 170

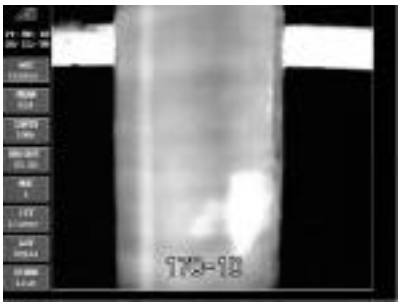

Inspection Data 1998
Area of Indications 167 cm^2

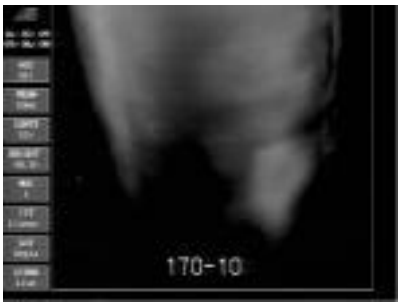

Inspection Data 2000
Area of Indications 174 cm^2

Column 4 Bent 184

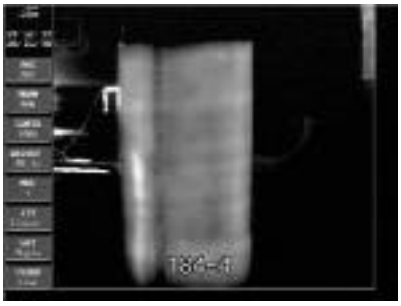

Inspection Data 1998
Area of Indications 131 cm^2

Inspection Data 2000
Area of Indications 105 cm^2

Column 5 Bent 184

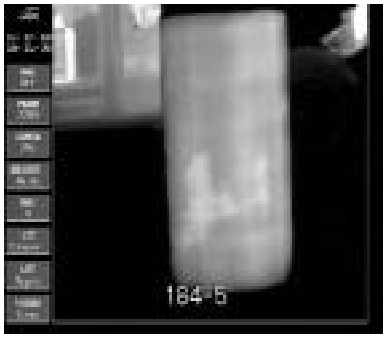

Inspection Date 1998
Area of Indication 225 cm^2

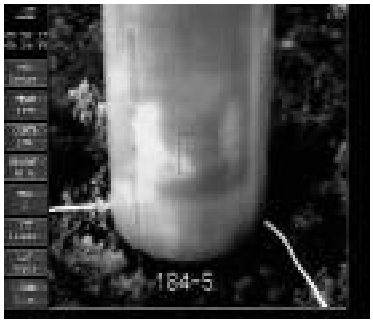

Inspection Date 1999
Area of Indication 215 cm^2

Inspection Date 2000
Area of Indication 223 cm^2

Column 6 Bent 184

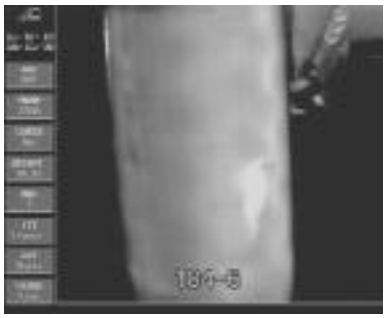

Inspection Date 1998
Area of Indication 66 cm^2

Inspection Date 1999
Area of Indication 60 cm^2

Inspection Date 2000
Area of Indication 70 cm^2